ANTIOXIDANTS & REDOX SIGNALING
Volume 23, Number 2, 2015

DOI: 10.1089/ars.2014.6094

Therapeutics

ORIGINAL RESEARCH COMMUNICATION

Hydrogen Sulfide Targets the Cys320/Cys529 Motif in Kv4.2 to Inhibit the I_{to} Potassium Channels in Cardiomyocytes and Regularizes Fatal Arrhythmia in Myocardial Infarction

Shan-Feng Ma,[1,2,*] Yan Luo,[1,*] Ying-Jiong Ding,[1] Ying Chen,[1] Shi-Xin Pu,[1] Hang-Jing Wu,[3] Zhong-Feng Wang,[3] Bei-Bei Tao,[1] Wen-Wei Wang,[1] and Yi-Chun Zhu[1]

Abstract

Aims: The mechanisms underlying numerous biological roles of hydrogen sulfide (H_2S) remain largely unknown. We have previously reported an inhibitory role of H_2S in the L-type calcium channels in cardiomyocytes. This prompts us to examine the mechanisms underlying the potential regulation of H_2S on the ion channels. ***Results:*** H_2S showed a novel inhibitory effect on I_{to} potassium channels, and this effect was blocked by mutation at the Cys320 and/or Cys529 residues of the Kv4.2 subunit. H_2S broke the disulfide bridge between a pair of oxidized cysteine residues; however, it did not modify single cysteine residues. H_2S extended action potential duration in epicardial myocytes and regularized fatal arrhythmia in a rat model of myocardial infarction. H_2S treatment significantly increased survival by $\sim$1.4-fold in the critical 2-h time window after myocardial infarction with a protection against ventricular premature beats and fatal arrhythmia. However, H_2S did not change the function of other ion channels, including I_{K1} and I_{Na}. ***Innovation and Conclusion:*** H_2S targets the Cys320/Cys529 motif in Kv4.2 to regulate the I_{to} potassium channels. H_2S also shows a potent regularizing effect against fatal arrhythmia in a rat model of myocardial infarction. The study provides the first piece of evidence for the role of H_2S in regulating I_{to} potassium channels and also the specific motif in an ion channel labile for H_2S regulation. *Antioxid. Redox Signal.* 23, 129–147.

Introduction

SEVERE CARDIAC ARRHYTHMIA, including ventricular tachycardia and fibrillation, is a major cause of death in the acute phase of myocardial infarction (21). About 20%–25% of the patients are attacked by fatal arrhythmia, including premature beats, ventricular tachycardia, and fibrillation within 24 h after an acute myocardial infarction (28, 42). This causes about 20,000 to 25,000 deaths each year in industrialized countries (1, 42, 45). The most effective therapy for acute myocardial infarction is percutaneous coronary intervention (PCI). However, it takes longer than 2 h on average before a patient would be helped by PCI after heart attack even in countries with the most efficient healthcare system (4). Effective prevention and treatment of fatal arrhythmia in this critical door-to-balloon time window would save numerous lives worldwide.

Innovation

The study provides the first piece of evidence for the role of hydrogen sulfide (H_2S) in regulating I_{to} potassium channels. A molecular switch labile for H_2S regulation is also identified in this ion channel, and this sheds some light on the discovery of the mechanisms underlying H_2S effects. Moreover, H_2S shows potent regularizing effects in an experimental model of acute myocardial infarction that has potential translational values.

[1]Shanghai Key Laboratory of Bioactive Small Molecules and Research Center on Aging and Medicine, Department of Physiology and Pathophysiology, Fudan University Shanghai Medical College, Shanghai, China.
[2]Department of Physiology, Bengbu Medical College, Bengbu, China.
[3]Institutes of Brain Science, Institute of Neurobiology and State Key Laboratory of Medical Neurobiology, Fudan University Shanghai Medical College, Shanghai, China.
*These authors contributed equally in this study.

Lidocaine is the current first-line drug that is used to prevent and treat fatal arrhythmia such as ventricular tachycardia and fibrillation in this time window (33). Lidocaine inhibits the sodium channel (I_{Na} channel) and attenuates phase 0 depolarization of the action potential in all fast responsive cells, including neurons and cardiomyocytes. Lidocaine inhibits depolarization of neurons in both central and peripheral nervous systems in addition to an inhibition of the ectopic pacemakers that appear in ischemic myocardium due to its nonselective inhibition on I_{Na} channels in both neurons and cardiomyocytes (2, 16). This gives rise to a hypothesis that some drugs that are more selective for cardiomyocytes than neurons would provide more specific cardioprotection against fatal arrhythmia with less side effects in neurons and other fast responsive cells.

Since hydrogen sulfide (H_2S) provides cardioprotection, including inhibition of L-type calcium channels (37), limitation of infarct size, and a decrease in cardiomyocytes apoptosis in ischemia/reperfusion injury (43), we aim at examining whether H_2S would show protection against fatal arrhythmia in the very acute phase of myocardial infarction. Theoretically, extension of the repolarization period of the action potential in cardiomyocytes would be another approach to extend the refractory period and provide protection against arrhythmia. While several potassium channels are involved in all phases of repolarization of the action potential (14, 34, 38), this prompts us to examine the effect of H_2S on potassium channels in cardiomyocytes.

H_2S has been shown to regulate the function of some ion channels, including the K_{ATP} channels in the vascular smooth muscles (44), L-type calcium channels in the cardiomyocytes (37) and vascular smooth muscles cells (40), T-type calcium channels in the sensory neurons (29), and the ATP-sensitive, intermediate-conductance, and small-conductance potassium channels in the vascular smooth muscles (25). However, the role of H_2S in regulating potassium channels in the cardiomyocytes is unknown. Our previous work shows that exogenous H_2S has no effect on K_{ATP} channels in cardiomyocytes at sodium hydrosulfide (NaHS; an H_2S donor) concentrations of 50 and 100 μM (37). To date, there is no direct evidence showing any effect of H_2S in the regulation of potassium channels in cardiomyocytes. The potassium channels in the cardiomyocytes play pivotal roles in cardiac electrophysiology and related diseases, including various types of arrhythmia (27). Whether H_2S has a role in regulating the potassium channels in the cardiomyocytes is proving to be an important question in the field of H_2S biology. Three major types of voltage-gated potassium channels are involved in the regulation of resting potential and action potential in cardiomyocytes (6). The inward rectifier K^+ channel (I_{K1}) is involved in the regulation of resting potential of the cell membrane (12), while potassium channels, including the transient outward K^+ channels (I_{to}), I_{K1}, and delayed rectifier K^+ channels (I_K), are involved in repolarization of action potential (6). Specifically, I_{to} channel regulates the outward K^+ currents during the phase 1 repolarization period and determines the velocity and duration of this phase. The I_{K1}, I_K, and long-lasting Ca^{2+} channels are involved in phase 2 repolarization. However, phase 3 repolarization is mainly induced by outward K^+ currents mediated by I_K channels (9). Therefore, factors that regulate specific K^+ channels would change either the resting potential or the repolarization course of the action potential in cardiomyocytes. These factors may regulate the excitability of the cardiomyocytes and the duration of the refractory period, thereby affecting the occurrence of cardiac arrhythmia. In this study, we aim at examining whether H_2S can regulate some specific potassium channels that determine the resting potential and the repolarization course of the action potential in cardiomyocytes.

In addition, despite numerous biological effects of H_2S that have been reported to date, the mechanisms underlying the H_2S actions remain largely unknown. We have recently shown that the disulfide bond formed between the Cys1024 and Cys1045 cysteine pair serves as a molecular switch for H_2S to regulate the conformation and function of vascular endothelial growth factor type 2 receptor (VEGFR2) (39). This prompts us to examine whether there is a certain cysteine pair that may serve as a molecular switch for H_2S to directly regulate the function of an ion channel and, subsequently, regulate the electrophysiology of cardiomyocytes.

Results

H_2S inhibits transient outward potassium channels in cardiomyocytes

Transient outward potassium current (I_{to}) was decreased after bath application of NaHS at 50 μM in epicardial myocytes at a membrane potential of 20, 30, 40, 50, and 60 mV (Fig. 1A, C). However, NaHS treatment did not cause a significant change in I_{to} in endocardial myocytes at a membrane potential from -30 to $+60$ mV (Fig. 1B, D). The effects of NaHS on inhibiting I_{to} in epicardial myocytes were more pronounced than those in endocardial myocytes (Fig. 1E). NaHS treatment (50 μM) did not change the steady-state outward current (I_{ss}) in epicardial myocytes nor in endocardial myocytes (Supplementary Fig. S1; Supplementary Data are available online at www.liebertpub.com/ars).

In epicardial myocytes, recorded at a membrane potential of $+60$ mV, the inhibition on I_{to} occurred at 3 min after bath application of NaHS at a concentration of 50 μM. At a higher concentration of 100 μM, the inhibition on I_{to} occurred within 2 min after NaHS application. The inhibitory effects lasted throughout the rest of the recording period of 14 min, which could not be washed out completely (Fig. 1F). These effects were concentration dependent as illustrated with a significant decrease in I_{to} by $25.30\% \pm 3.461\%$, $45.82\% \pm 5.301\%$, and $51.67\% \pm 4.318\%$ at concentrations of 50, 100, and 200 μM as compared with those of the vehicle-treated group at 5 min after NaHS application (Fig. 1G).

The effects of NaHS application at 50 μM on the steady-state activation of I_{to} channels in epicardial myocytes are shown in Figure 1H. With a holding potential of -80 mV, I_{to} was elicited by 500 ms depolarizing pulses between -40 and $+80$ mV. The activation curves were fitted by the Boltzman equation: $G/G_{max} = 1/[1 + \exp(V_T - V_{1/2}/K)]$, where G/G_{max} represents the ratio of present conductance to the maximum conductance and V_T represents the values of the depolarizing pulses. $V_{1/2}$ (a half-maximum inactivation potential) values of the curves were 21.24 ± 1.59 and 25.05 ± 1.85 mV in the vehicle-treated group and the NaHS-treated group, respectively. K values were 12.69 ± 0.77 and 16.19 ± 0.89 ($p < 0.05$ *vs.* the vehicle-treated group) in the vehicle-treated group and the NaHS-treated group, respectively. NaHS treatment did not cause any significant difference in the steady-state

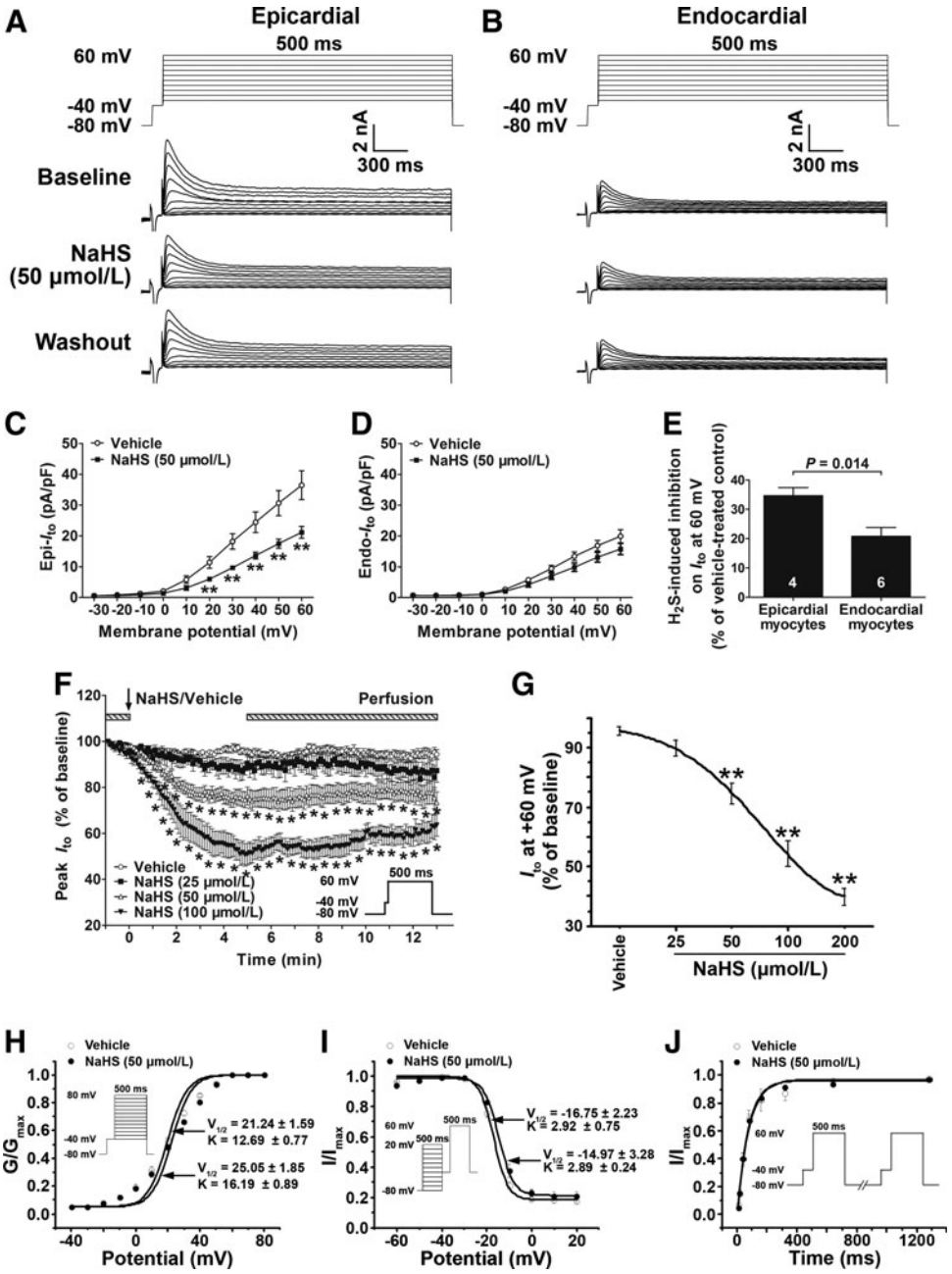

FIG. 1. H_2S inhibits transient outward potassium currents (I_{to}) in epicardial but not endocardial myocytes isolated from SD rats. **(A, B)** Representative traces of I_{to} in an epicardial **(A)** or an endocardial **(B)** myocyte treated with NaHS at 50 μM. **(C, D)** Average *I–V* relation curves of I_{to} of epicardial **(C)** and endocardial **(D)** myocytes treated with NaHS (50 μM) or vehicle for 5 min ($n = 6$). **(E)** Comparison of the H_2S effects in epicardial and endocardial myocytes. **(F)** Time course of peak I_{to} in epicardial myocytes treated with vehicle or NaHS (25, 50 or 100 μM) ($n = 8$, 6, 10, 10). **(G)** Concentration-response curves of peak I_{to} in epicardial myocytes treated with vehicle or NaHS at 25, 50, 100, or 200 μM ($n = 8$, 6, 10, 11, 6). I_{to} was quantified by subtracting the current at the end of the voltage pulse from the peak current. **(H–J)** NaHS treatment (50 μM) has no effect on the steady-state activation **(H)**, inactivation **(I),** and recovery after inactivation **(J)** of epi-I_{to} channel ($n = 6$). Values are means ± SEM. $^*p < 0.05$, $^{**}p < 0.01$ *versus* the vehicle-treated group. H_2S, hydrogen sulfide; NaHS, sodium hydrosulfide; SD, Sprague–Dawley.

activation curve of I_{to} channels in epicardial myocytes at a concentration of 50 μM.

The effect of NaHS on the steady-state inactivation of I_{to} channels in epicardial myocytes is shown in Figure 1I. The experiments were performed using a two-pulse protocol containing a 500 ms pulse between −100 and +40 mV with an interval of 10 ms and after a 500 ms test pulse to +60 mV from a holding potential of −80 mV. The curves were fitted by the Boltzman equation: $I/I_{max} = 1/[1 + \exp(V_T - V_{1/2}/K)]$, where I/I_{max} represents the ratio of the current to the maximum current and V_T represents the values of the depolarizing potential of the prepulses. $V_{1/2}$ values were −16.75 ± 0.91 and −14.97 ± 1.34 mV in the vehicle-treated group and the NaHS-treated group, respectively. *K* values were 2.92 ± 0.31 and 2.89 ± 0.10 in the vehicle-treated group and the NaHS-treated group, respectively. NaHS treatment did not cause a significant difference in the steady-state inactivation curve of I_{to} epicardial myocytes at a concentration of 50 μM.

Figure 1J shows the effect of NaHS treatment on the kinetics of recovery of I_{to} from inactivation in epicardial myocytes. At a holding potential of −80 mV, the cells were stimulated with a double-pulse protocol containing a 500 ms condition pulse to +60 mV followed by a 500 ms test pulse to +60 mV with increasing intervals of 10, 20, 40, 80, 160, 320, 640, 1280, and 2560 ms. An increase in the interval between the condition pulse and the test pulse resulted in a recovery of I_{to}, which was fitted by the exponential equation: $I/I_{max} = 1 - \exp(-t/\tau)$, in which *t* means the values of the interval and τ means the time constant of I_{to} recovery from inactivation. The τ values were 53.16 ± 4.39 and 62.59 ± 6.51 ms in the vehicle-treated group and the NaHS-treated group, respectively. Bath application of NaHS (50 μM) did not induce a shift of the recovery curve of I_{to}.

The Kv4.2 subunit of the I_{to} channel serves as a direct target molecule for H_2S to inhibit the I_{to} current

I_{to} current was not detected in naive HEK293 cells with whole-cell recording (Fig. 2A). I_{to} current was recorded in HEK293 cells transfected with vectors expressing the Kv4.2 subunit alone (Fig. 2A). Larger I_{to} currents were recorded in the cells co-expressing the Kv4.2 subunit and the K_v channel interacting protein 2 (KChIP2) subunit (Fig. 2A, B). NaHS treatment caused a significant inhibition in I_{to} current in both the cells expressing the Kv4.2 subunit (Fig. 2A, C, D) and the cells co-expressing the Kv4.2 and KChIP2 units (Fig. 2A, E, F) at concentrations of 50 and 100 μM. This current was confirmed as I_{to} current by an inhibition induced by the I_{to} channel blocker, 4-aminopyridine (4-AP, 4 mM) (Fig. 2A).

Mutation at Cys320 and/or Cys529 causes a decrease in basal I_{to} current and blocks the effects of H_2S in inhibiting the I_{to} channels

The I_{to} channels with mutations at Cys320 and/or Cys529 of its Kv4.2 subunit were successfully expressed on the cell membrane with a cellular distribution pattern similar to the wild-type Kv4.2/KChIP2 I_{to} channels (Fig. 3A). Basal I_{to} current was significantly decreased in the cells expressing I_{to} channels with mutations at the Cys320 or the Cys529 sites of the Kv4.2 unit as compared with the cells expressing wild-

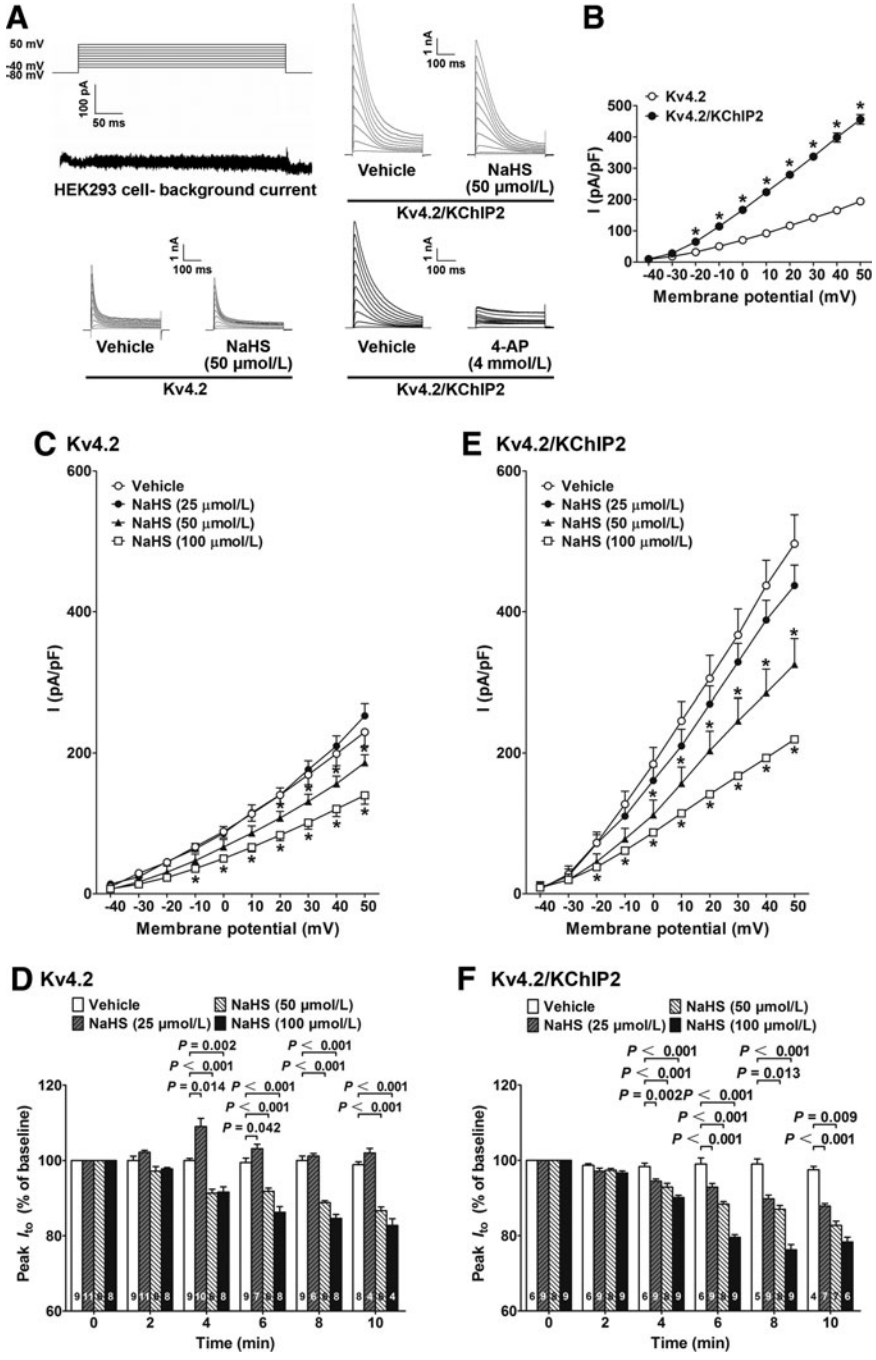

FIG. 2. The Kv4.2 subunit is the direct target molecule for H_2S to regulate I_{to} current. **(A)** Representative traces showing the background current in naive HEK293 cells, and I_{to} currents recorded in HEK293 cells expressing recombinant Kv4.2 subunit with or without the KChIP2 subunit. **(B)** Larger I_{to} currents were recorded in the cells co-expressing the Kv4.2 and KChIP2 subunit as compared with the cells expressing Kv4.2 alone. **(C, D)** The concentration-response curve **(C)** and the time course **(D)** of I_{to} with NaHS treatment in the cells expressing the Kv4.2 subunit. **(E, F)** The concentration-response curve **(E)** and the time course **(F)** of I_{to} with NaHS treatment in the cells co-expressing the Kv4.2 and KChIP2 units. Values are means ± SEM. $^*p < 0.05$ versus the Kv4.2 group **(B)** and the vehicle-treated group **(C** and **E)**.

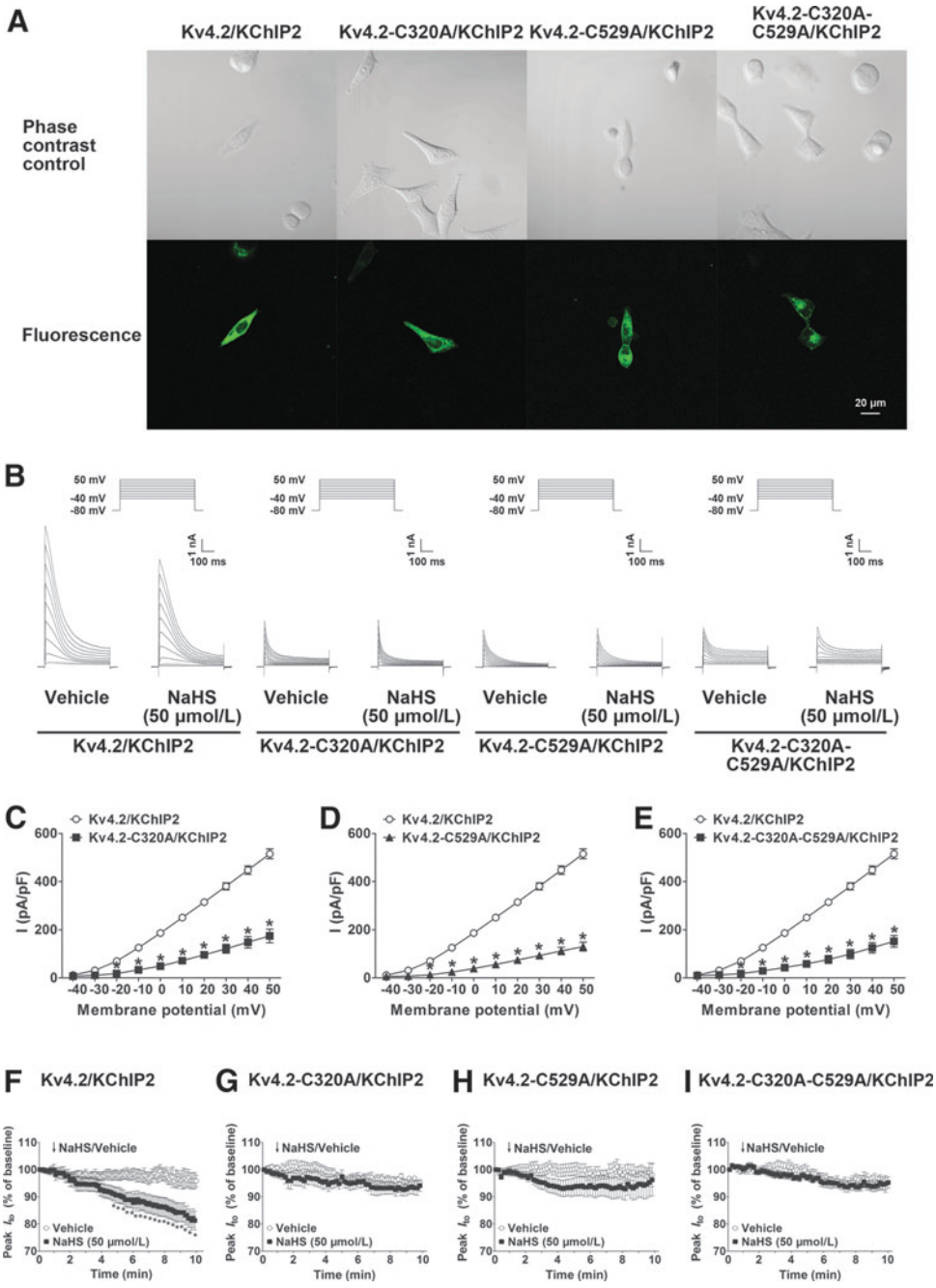

FIG. 3. The Cys320/Cys529 motif in Kv4.2 is essential to regulate I_{to} current. (A) Confocal microscopy showing expression of wild-type Kv4.2/KChIP2 and mutant Kv4.2, including Kv4.2-C320A/KChIP2, Kv4.2-C529A/KChIP2, or Kv4.2-C320A-C529A/KChIP2. *Green* color indicates the fluorescent signals of the Kv4.2-GFP-fusion gene expressed in the HEK293 cells. **(B)** Representative traces showing I_{to} current recorded in the cells expressing wild-type Kv4.2/KChIP2 and mutant Kv4.2, including Kv4.2-C320A/KChIP2, Kv4.2-C529A/KChIP2, or Kv4.2-C320A-C529A/KChIP2 in the presence or absence of NaHS (50 μM). **(C–E)** Basal I_{to} current was significantly decreased in the cells expressing I_{to} channels with a mutation at Cys320 **(C)**, Cys529 **(D),** or both Cys320 and Cys529 **(E)**. **(F–I)** NaHS treatment (50 μM) caused an immediate and significant decrease in I_{to} current in the cells expressing wild-type Kv4.2/KChIP2 **(F)** but not in the cells expressing mutant Kv4.2 subunits, that is, Kv4.2-C320A/KChIP2 **(G)**, Kv4.2-C529A/KChIP2 **(H),** or Kv4.2-C320A-C529A/KChIP2 **(I)**.

type I_{to} channels (Fig. 3B–D). NaHS treatment (50 μM) caused an immediate and significant decrease in I_{to} current in the cells expressing wild-type Kv4.2/KChIP2 but not in the cells expressing mutant Kv4.2 subunits, that is, Kv4.2-C320A/KChIP2 or Kv4.2-C529A/KChIP2 (Fig. 3B, F–H).

In addition, a double mutation at both the Cys320 and Cys529 sites in Kv4.2 was also created. Basal I_{to} current was significantly decreased in the cells expressing Kv4.2-C320A-C529A/KChIP2 as compared with the cells expressing wild-type Kv4.2/KChIP2 (Fig. 3B, E). Likewise, NaHS treatment (50 μM) did not cause any decrease in I_{to} current in the cells expressing the I_{to} channels with a double mutation at the Cys320 and Cys529 sites in Kv4.2 (Fig. 3B, I).

The experiments mentioned earlier were also repeated in the cells transfected with Kv4.2 or its mutant alone without KChIP2. Likewise, mutation at Cys320, Cys529, or the double mutation at Cys320 and Cys529 caused a decrease in basal I_{to} current and (Fig. 4A–D), and H_2S-induced inhibition on I_{to} current was blocked in the cells expressing Kv4.2-C320A, Kv4.2-C529A, or Kv4.2-C320A-C529A (Fig. 4A, E–H). The data indicate that H_2S-induced regulation on Kv4.2 is independent of the auxiliary subunit KChIP2.

Mutation at Cys133, Cys231, Cys236, Cys530, Cys390, Cys484, Cys588, Cys503, or Cys583 of the Kv4.2 subunit does not block the inhibitory regulation of H_2S on I_{to} current

NaHS treatment (50 μM) caused a decrease in I_{to} current in the cells expressing Kv4.2-C133A/KChIP2, Kv4.2-C231A/

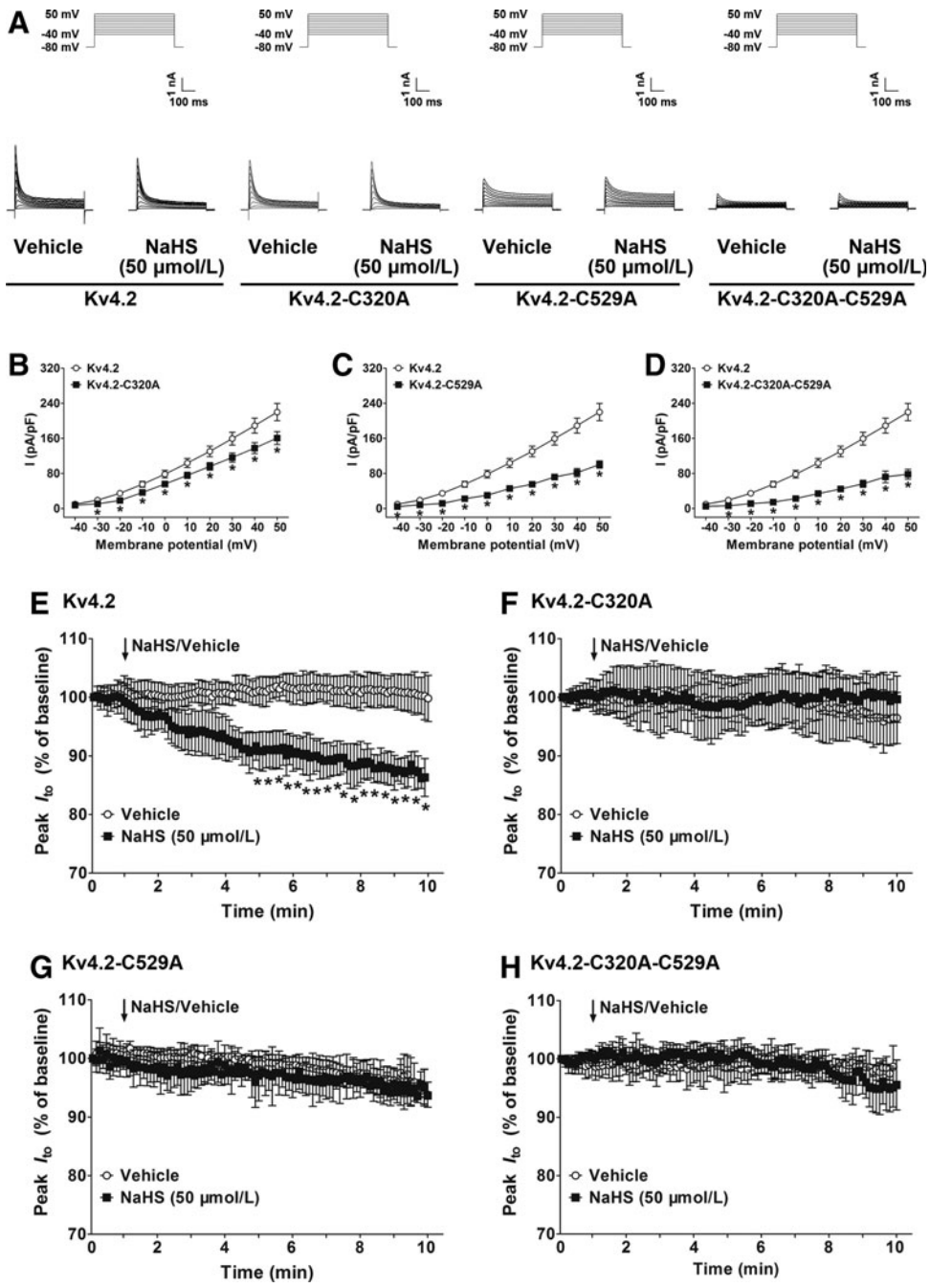

FIG. 4. H_2S has no effect on mutant Kv4.2 without co-expression of KChIP2. **(A)** Representative traces showing I_{to} current recorded in the cells expressing wild-type Kv4.2 and mutant Kv4.2, including Kv4.2-C320A, Kv4.2-C529A, or Kv4.2-C320A-C529A in the presence or absence of NaHS (50 μM). **(B–D)** Basal I_{to} current was significantly decreased in the cells expressing I_{to} channels with a mutation at Cys320 **(B)**, Cys529 **(C),** or both Cys320 and Cys529 **(D)**. **(E–H)** NaHS treatment (50 μM) caused an immediate and significant decrease in I_{to} current in the cells expressing wild-type Kv4.2 **(E)** but not in the cells expressing mutant Kv4.2 subunits, that is, Kv4.2-C320A **(F)**, Kv4.2-C529A **(G),** or Kv4.2-C320A-C529A **(H)**. Values are means ± SEM. $^*p < 0.05$ versus the Kv4.2 group **(B–D)** and the vehicle-treated group **(E)**.

KChIP2, Kv4.2-C236A/KChIP2, Kv4.2-C530A/KChIP2, Kv4.2-C390A/KChIP2, Kv4.2-C484A/KChIP2, Kv4.2-C588A/KChIP2, Kv4.2-C503A/KChIP2, or Kv4.2-C583A/KChIP2 (Fig. 5B–J). The inhibitory effects of NaHS treatment (50 μM) on these mutant I_{to} potassium channels are similar to those observed in the cells expressing wild-type I_{to} channels (Kv4.2/KChIP2) (Fig. 5A).

Interestingly, these mutations caused different changes in basal I_{to} current in the absence of NaHS. Mutation at the Cys133, Cys231, Cys236, or Cys530 sites caused a decrease in basal I_{to} current (Fig. 5L). In contrast, mutation at the Cys390 or Cys484 caused an increase in basal I_{to} current as compared with that of the wild-type channels (Fig. 5L). However, basal I_{to} current was not changed in the cells expressing Kv4.2-C588A/KChIP2, Kv4.2-C503A/KChIP2, or Kv4.2-C583A/KChIP2 (Fig. 5L).

Mutation at Cys132 of the Kv4.2 subunit turns over the inhibitory effect of H_2S on I_{to} channels into a stimulating effect

The basal I_{to} current was decreased in the cells expressing Kv4.2-C132A/KChIP2 as compared with the cells expressing wild-type Kv4.2/KChIP2 (Fig. 5L). This effect of mutation at Cys132 on basal I_{to} current was similar to that of the mutation at Cys133, Cys231, Cys236, or Cys530 (Fig. 5L). However, NaHS treatment (50 μM) caused an unexpected increase in I_{to} current in contrast to an inhibition in I_{to} current induced by

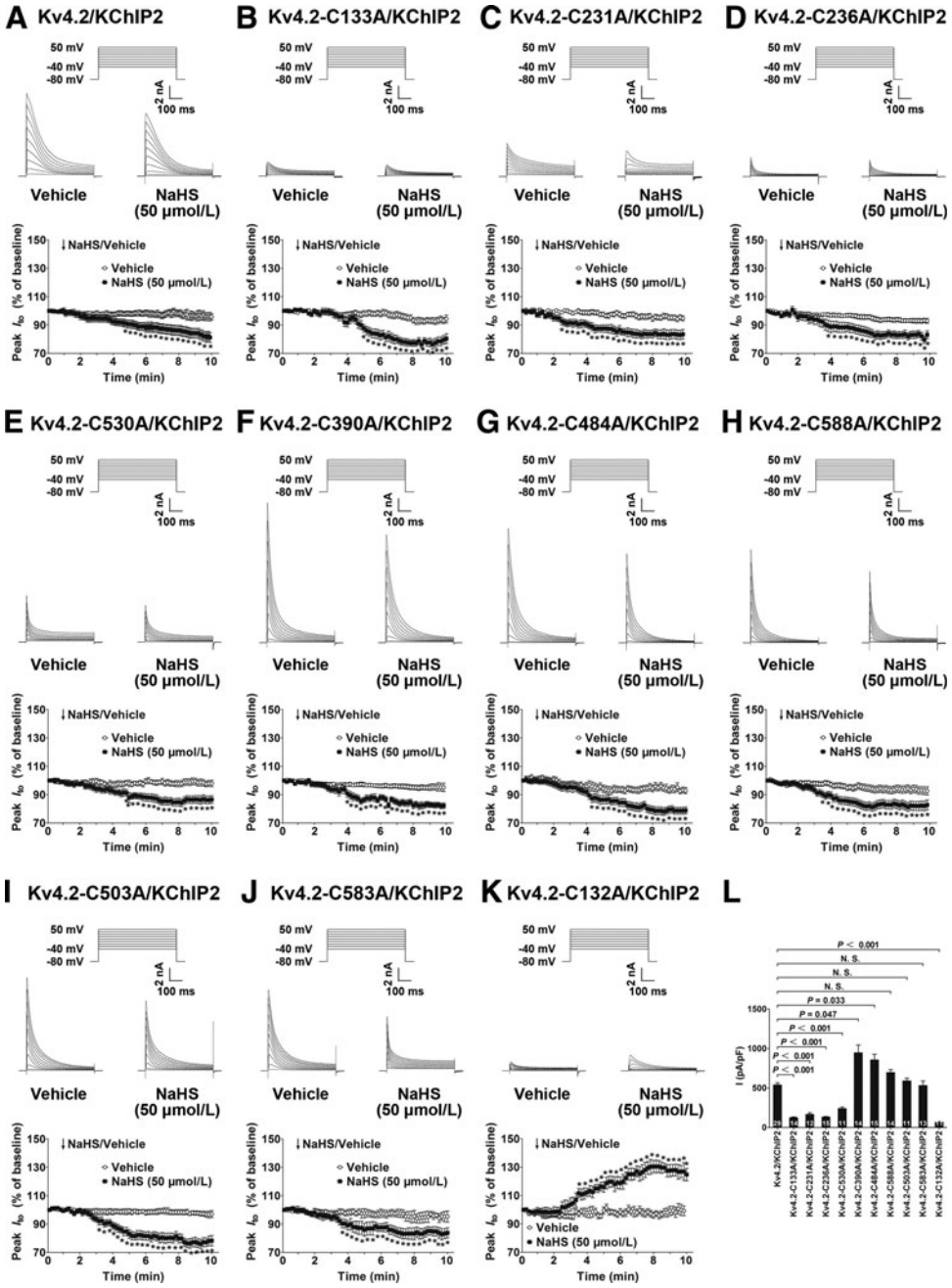

FIG. 5. Role of Cys133, Cys231, Cys236, Cys530, Cys390, Cys484, Cys588, Cys503, Cys583, or Cys132 in regulating the basal function of the Kv4.2 subunit and in mediating the effects of H_2S in regulating Kv4.2 function. (A–K) Effects of NaHS treatment in the cells expressing wild-type Kv4.2 **(A)** or mutant Kv4.2 with mutations at Cys133 **(B)**, Cys231 **(C)**, Cys236 **(D)**, Cys530 **(E)**, Cys390 **(F)**, Cys484 **(G)**, Cys588 **(H)**, Cys503 **(I)**, Cys583 **(J),** or Cys132 **(K)**. **(L)** Graphs showing effects of mutations at the earlier mentioned cysteine sites on basal I_{to} current mediated *via* Kv4.2. Values are means ± SEM. $*p < 0.05$ versus the Kv4.2 group **(B)** and the vehicle-treated group **(C** and **E)**.

H_2S in the cells expressing wild-type Kv4.2/KChIP2 (Fig. 5A, K).

H_2S cleaves the disulfide bonds but does not modify the free cysteine residues

A model peptide containing a disulfide bridge linking two peptides (α and β peptide) each contains a cysteine residue and with a sequence identical to the regions of Cys320 and Cys529 in the Kv4.2 molecule was examined with ESI-CID-MS-MS analysis where a disulfide bond was identified between the α and β peptides. A precursor ion molecule of $[M+2]^{2+}$ *m/z* 746.32 (the combined α and β peptides) yielded a series of collision-induced dissociation (CID) fragments that matched with the CID-induced y ions of both the α and β peptides, that is, y_3 ion of the α peptide $([M+H]^+$ *m/z* 306.18), y_2 ion of the β peptide ($[M+H]^+$ *m/z* 262.19), and y_3 ion of the β peptides ($[M+H]^+$ *m/z* 365.21) (Fig. 6A). This illustrates that these two peptides are joined together by a covalent bond. Moreover, Figure 6A showed an additional series of CID-induced y ions containing the Cys residue linking with another peptide by a disulfide bond, including y_4 ions of the α peptide bound with the β peptide ($[M+H]^+$ *m/z* 1163.41), the y_5 ions of the α peptide bound with the β peptide ($[M+H]^+$ *m/z* 1250.45), the y_6 ions of the α peptide bound with the β peptide ($[M+H]^+$ *m/z* 1378.54), the y_4 ions of β the peptide bound with teh α peptide ($[M+H]^+$ *m/z* 1202.49), the y_5 ions of the β peptide bound with the α peptide ($[M+H]^+$ *m/z* 1303.54), and the y_6 ions of the β peptide bound with the α peptide ($[M+H]^+$ *m/z* 1390.57).

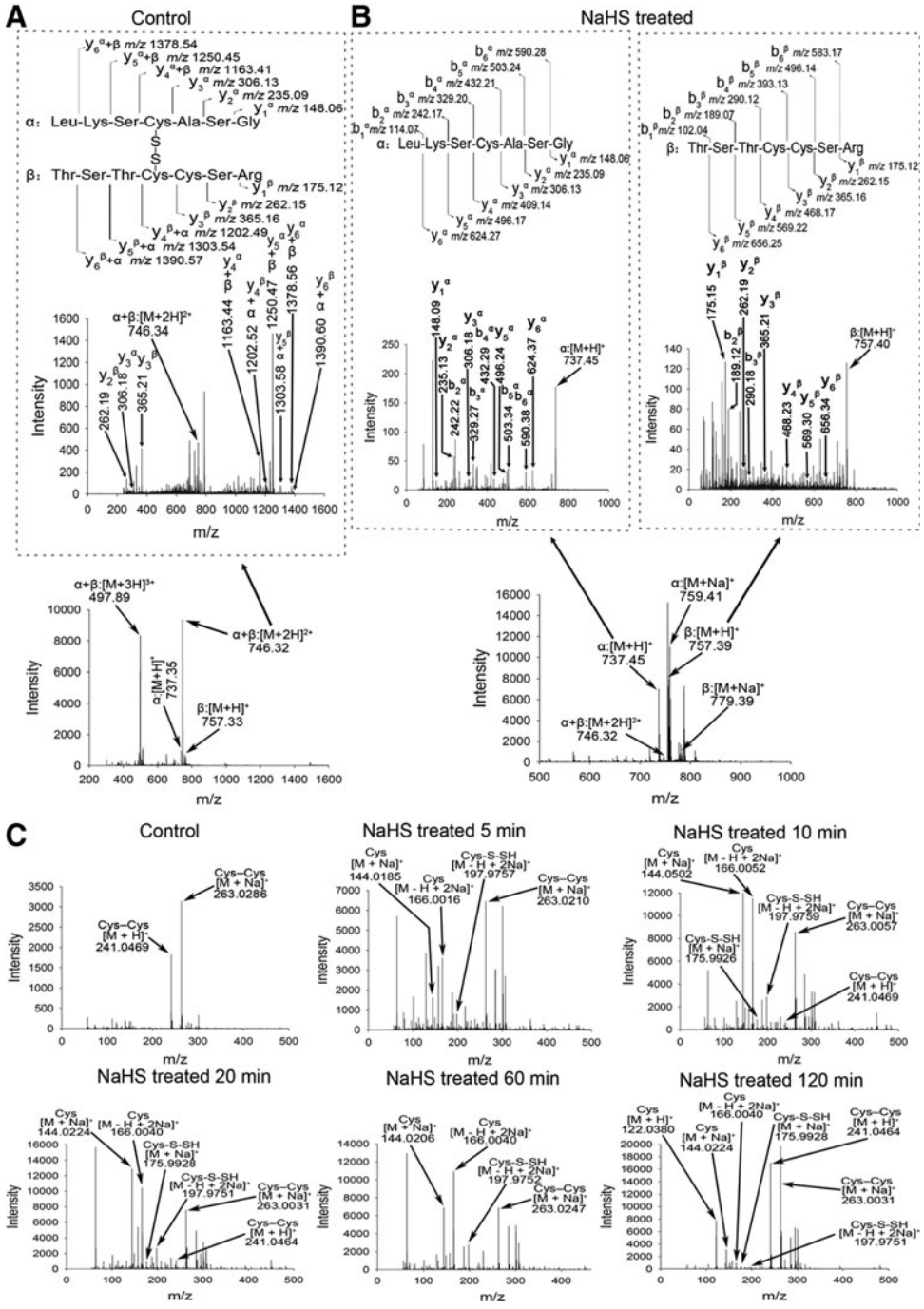

FIG. 6. H_2S treatment breaks the disulfide bond contained in the model peptides without chemical modification on free amino acid residues. **(A)** Tandem mass spectrometry of the precursor ion of the combined model peptide ($\alpha+\beta$) containing a disulfide bond, $[M+2H]^{2+}$ *m/z* 746.32, where a series of y ions was yielded from both the α and β peptides, and the fragments containing the disulfide bond were identified. **(B)** Tandem mass spectrometry of the combined model peptide ($\alpha+\beta$) containing a disulfide bond treated with H_2S where the combined model peptide was cleaved into two single peptides, α and β. The α peptide was identified as a precursor ion of $[M+H]^+$ *m/z* 737.45, which yielded a series of y and b ions of the α peptide. The β peptide was identified as a precursor ion of $[M+H]^+$ *m/z* 757.39, which yielded a series of y and b ions of the β peptide. **(C)** ESI mass spectrometry of the time course of a simple model peptide, Cys–Cys, which was treated with H_2S and a transient S-sulfhydrated intermediate (Cys–S–SH) was identified during the process of the cleavage of the disulfide bond. The peak level of this intermediate was found in 10 min after treatment. In 120 min, some disulfide bonds were spontaneously reformed. ESI, electrospray ionization.

These data further confirmed that the covalent bond was localized between the two cysteine residues (Cys320 and Cys529). Treatment of this combined peptide with H_2S caused breaking of the S–S bond between Cys320 and Cys529 as evidenced by ESI-CID-MS-MS analysis where the precursor ion molecule of the combined α and β disappeared and the single precursor ion molecules of the α ($[M+H]^+$ *m/z* 737.45) and β ($[M+H]^+$ *m/z* 757.39) peptides were identified (Fig. 6B). The single precursor ion molecules of the α and β peptides each yielded a series of CID fragments that matched with the sequence of peptide α and peptide β, respectively (Fig. 6B).

On the other hand, the single forms of peptide α and β were reacted, respectively, with H_2S to examine whether there was any modification in the free cysteine residues. No chemical modifications were found in these two single peptides on incubation with H_2S. In addition, a simpler model chemical, cystine (Cys–Cys) was treated with H_2S at different time points to examine the process of H_2S-induced breaking of a disulfide bond using ESI-MS. As shown in Figure 6C, the reaction of Cys–Cys with H_2S yielded cysteine (Cys), indicating breaking of the disulfide bond in 10 min when an intermediate (Cys – S – SH) was identified at its peak level (Fig. 6C). In 60 min, most Cys – Cys was cleaved into Cys and in 120 min, the intermediate was hardly identified (Fig. 6C). These data validate the two-step reaction formula for H_2S to cleave a disulfide bond where Cys – S – SH served as a

product of reaction 1 and served as a reactant for reaction 2 (39):

Reaction 1:

$$HS^- + C_3H_6NO_2\text{–}S\text{–}S\text{–}C_3H_6NO_2 \rightarrow C_3H_6NO_2\text{–}S^- + HS\text{–}S\text{–}C_3H_6NO_2$$

Reaction 2:

$$HS^- + HS\text{–}S\text{–}C_3H_6NO_2 \rightarrow C_3H_6NO_2\text{–}S^- + HS\text{–}SH$$

Two hours after H_2S treatment, some disulfide bonds were reformed to yield Cys–Cys again (Fig. 6C). All these data support the idea that H_2S targets and cleaves the disulfide bond between a pair of cysteine residues as a reversible process; however, H_2S does not modify the free $-SH$ groups of the cysteine residues or any other residues in these model molecules.

H_2S prolongs action potential duration and decreases the maximal velocity of repolarization of action potential in epicardial myocytes

Figure 7A shows representative traces of action potential in epicardial myocytes recorded before and 5 min after bath application of NaHS at 50 μM. Five minutes after bath application of NaHS at 50 μM, action potential durations (APD_{10}, APD_{20}, APD_{50}, APD_{90}) were increased as compared with those of the vehicle-treated group (124.94% ± 2.99% *vs.* 99.91% ± 1.66%, 119.34% ± 4.78% *vs.* 99.43% ± 1.62%, 115.46% ± 3.42% *vs.* 100.21% ± 1.48%, 116.63% ± 2.83% *vs.* 102.15% ± 2.03%, respectively) (Fig. 7B). However, $APD_{10–20}$, $APD_{20–50}$, and $APD_{50–90}$ were not significantly changed by NaHS treatment (50 μM) (Fig. 7C). Maximal velocity of repolarization ($-dV/dt_{max}$) was significantly decreased in the cells treated with NaHS at 50 μM as compared with the vehicle-treated group (-7.86 ± 1.01 *vs.* -26.85 ± 3.03, $p < 0.001$) (Fig. 7D).

In addition, other parameters of the action potential such as peak amplitude of the action potential, the maximal velocity of phrase 0 depolarization ($+dV/dt_{max}$), and the resting potential were not changed with NaHS treatment at 50 μM (Fig. 7E–G).

H_2S extends the refractory period in cardiomyocytes

Figure 7H and J shows representative traces of a cluster of action potentials that were provocated by eight basal stimulates with equal intervals followed by one conditional stimulate with evenly decreasing intervals to evaluate the refractory period, which is reflected by the interval between the last basal stimulate and the nearest conditional stimulate that evoked the closest premature action potential in the presence or absence of NaHS (50 μM). Five minutes after bath application of NaHS (50 μM), the refractory period was significantly increased as compared with that of the vehicle-treated group (Fig. 7I).

H_2S-induced inhibition in I_{to} is not dependent on cytoplasmic calcium

Pretreatment with the L-type calcium channel blocker, verapamil (20 μM) did not change basal I_{to} current, and the inhibitory effects of H_2S on I_{to} channels were not changed by pretreatment with verapamil (Fig. 8A, C, E). In contrast, pretreatment with a combination of verapamil (20 μM) and thapsigargin (2 μM) caused a significant decrease in basal I_{to} current by 51.7%, and NaHS treatment (50 μM) still showed an inhibitory effect on I_{to} channels (Fig. 8B, D, E). The inhibitory effects of H_2S on I_{to} channels in cardiomyocytes with or without calcium exhaustion were identical (Fig. 8F). These data illustrated that cytoplasmic calcium sensitizes the I_{to} channels in basal condition; however, H_2S-induced inhibition in I_{to} was not dependent on cytoplasmic calcium.

H_2S is a potent regularizing factor and significantly improves survival in acute myocardial infarction

Figure 9A shows representative electrocardiogram (ECG) recorded in the rats with acute myocardial infarction at baseline, with ischemia before treatment, or with ischemia 10 min after treatment. The rats were treated with NaHS at 12.5, 25, or 50 μmol/kg, with lidocaine at 7.5 mg/kg, or with vehicle by bolus intravenous injection. Statistical analysis showed that there were elevations of the ST segment in ECG in all groups after left anterior descending (LAD) ligation before treatment (Fig. 9B). This ST elevation was not changed at 10 min after vehicle treatment; however, that was significantly decreased in the groups treated with NaHS at 25 and 50 μmol/kg ($p = 0.016$ and $p = 0.007$ *vs.* that before treatment, respectively). However, lidocaine (7.5 mg/kg) did not show any significant effect on ST elevation compared with that before treatment (Fig. 9B).

The incidence of arrhythmia was about 77% in 10 min after coronary artery occlusion before treatment. There were various kinds of arrhythmia such as ventricular fibrillation and tachycardia, and premature beats, including singlets, couplets, triplets, and bigeminy. Incidence and severity of arrhythmia in all groups were assessed with a scoring system (11) using raw ECG data of each rat. There was no arrhythmia with a score 0 in all groups before LAD ligation, and the scores were about 2 in 10 min after coronary artery occlusion before treatment. In the vehicle-treated group, arrhythmia became more severe with a significant increase in arrhythmia scores at 2 h after treatment as compared with that before treatment ($p = 0.003$) (Fig. 9C). Interestingly, there was a dose-dependent amelioration of arrhythmia with a decrease in arrhythmia scores in all groups treated with NaHS at dosages of 12.5 and 25 μmol/kg as compared with that before treatment ($p = 0.009$ and 0.008, respectively) (Fig. 9C). Lidocaine treatment (7.5 mg/kg) also caused a decrease in arrhythmia scores as compared with that before treatment ($p = 0.012$) (Fig. 9C).

Further analysis of the raw data of ECG recording showed that treatment with NaHS decreased the incidence of the premature beats, including singlets, couplets, triplets, bigeminy, and trigeminy at dosages of 12.5 and 25 μmol/kg as compared with that before treatment ($p = 0.042$ and $p = 0.001$, respectively) (Fig. 9D). The time duration of these premature beats was also decreased in the group treated with NaHS at 25 μmol/kg as compared with that before treatment ($p = 0.005$) (Fig. 9E). Lidocaine treatment (7.5 mg/kg) also decreased both the incidence and the time duration of the premature beats as compared with that before treatment ($p = 0.018$, Fig. 9D; and $p = 0.023$, Fig. 9E; respectively). In contrast, the vasodilator, Regitine (125 μg/kg), showed no regularizing effects as compared with that before treatment (Fig. 9D, E). Moreover, the incidence of fatal arrhythmia, including ventricular tachycardia and fibrillation, was decreased in the groups treated with NaHS at dosages of 12.5

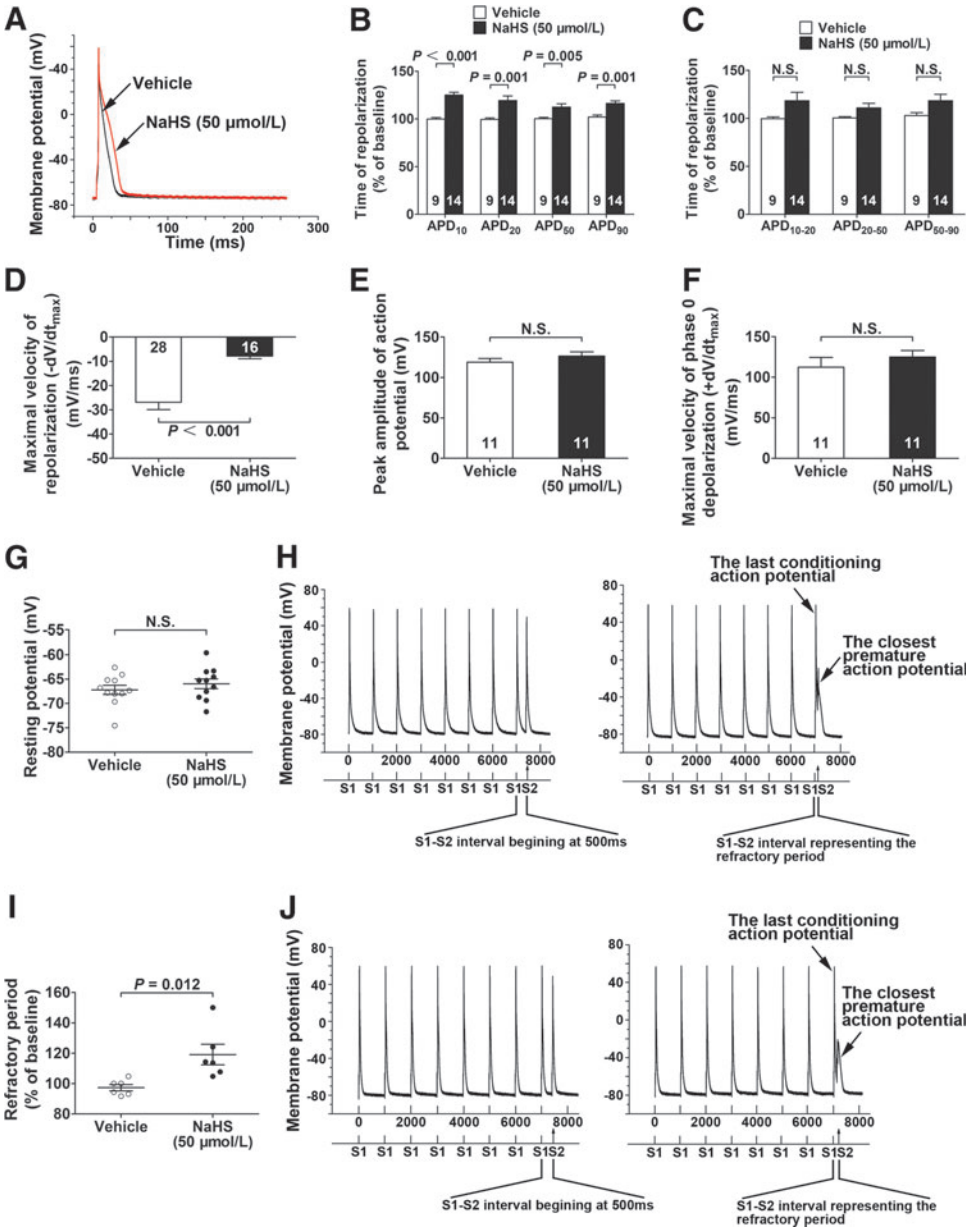

FIG. 7. H_2S treatment extends APD, reduces the maximal velocity of repolarization of action potential, and extends the refractory period in epicardial myocytes isolated from SD rats. **(A)** Representative traces of action potential recorded in epicardial myocytes at 5 min after bath application of NaHS (50 μM) or vehicle. **(B)** Mean values of the time from peak depolarization to 10%, 20%, 50%, and 90% repolarization of the action potential (APD_{10}, APD_{20}, APD_{50}, and APD_{90}). **(C)** Mean values of the time from 10%, 20%, and 50% repolarization to 20%, 50%, and 90% repolarization of the action potential, respectively ($APD_{10–20}$, $APD_{20–50}$, and $APD_{50–90}$). **(D)** NaHS treatment (50 μM) reduced maximal velocity of repolarization, which was observed at early repolarization phase. **(E, F)** NaHS treatment changed neither peak amplitude of action potential **(E)** nor the maximal velocity of phase 0 depolarization **(F)**. **(G)** The resting membrane potential was not changed by NaHS treatment (50 μM). **(H, J)** Representative traces of action potential elicited with a train of eight conditioning pulses (S1) followed by a premature pulse (S2) that was progressively closer with 1 ms steps in each set of the tests in the cardiomyocytes treated with vehicle **(H)** or NaHS at 50 μM **(J)**. **(I)** Mean values of the refractory period of the cardiomyocytes treated with vehicle or NaHS at 50 μM. Values are means ± SEM. A p-value < 0.05 was considered statistically significant. APD, action potential durations.

and 25 μmol/kg as compared with that before treatment ($p = 0.008$ and $p = 0.017$, respectively) (Fig. 10A, B). Likewise, the time duration of these fatal arrhythmia was also decreased with NaHS treatment at dosages of 12.5 and 25 μmol/kg as compared with that before treatment ($p = 0.028$ and $p = 0.009$, respectively) (Fig. 10A, C).

To examine the potential effects of blood pressure on the regularizing effects of these agents, blood pressure was measured in these groups. Bolus injection of NaHS (25 μmol/kg) caused a transient decrease in blood pressure, which peaked in 3 min and recovered in 6 min (Fig. 10D). Regitine decreased blood pressure for 30 min and this decrease also

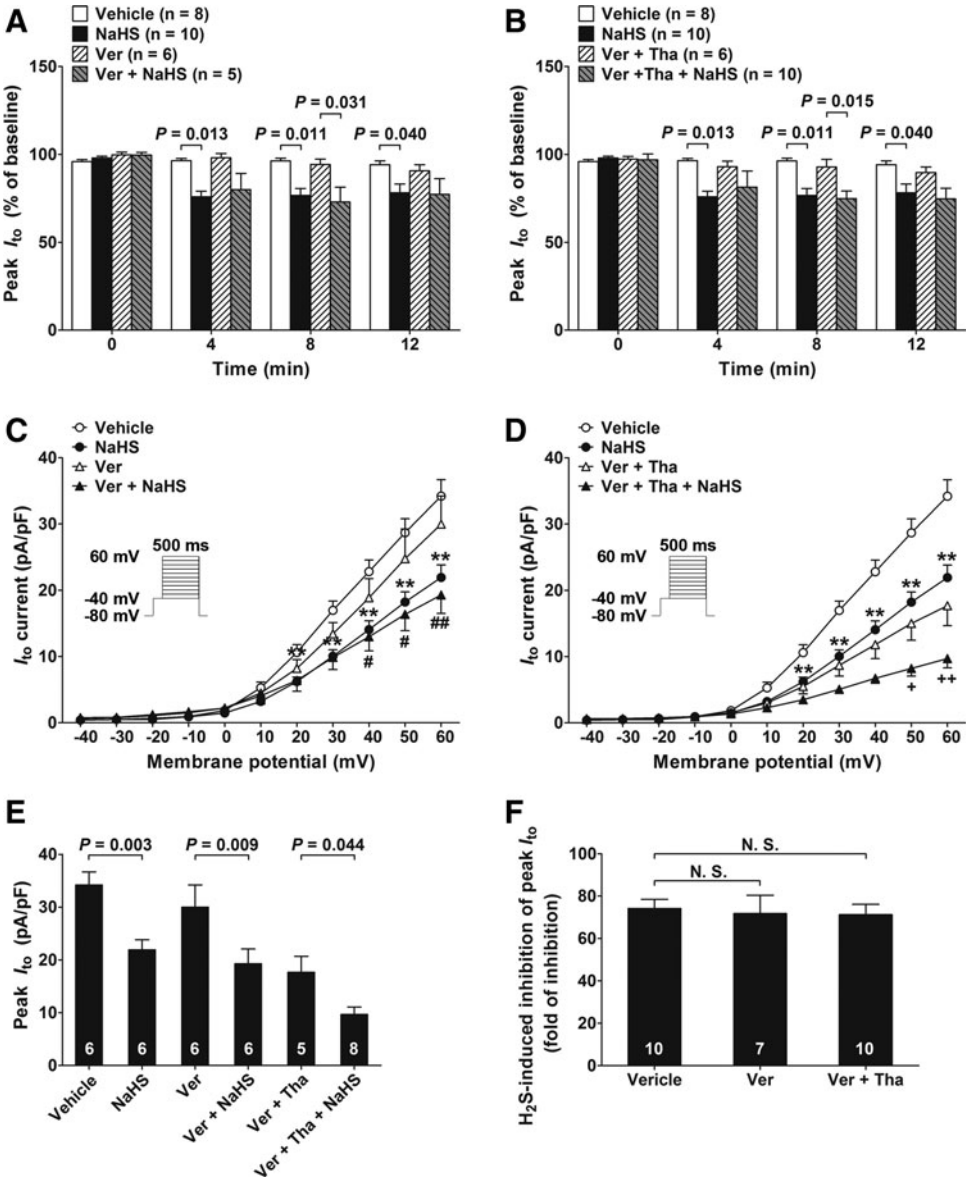

FIG. 8. Influence of $[Ca^{2+}]_i$ on NaHS-induced inhibition on I_{to} of epicardial myocyte isolated from SD rats. (A–D) Ver had no effect on I_{to}; meanwhile, NaHS decreased I_{to}, and this effect was not blocked by Ver **(A, C)**. In contrast, pretreatment with combination of Ver and Tha caused a significant decrease in basal I_{to} current by 51.7%, and NaHS still showed an inhibitory effect on I_{to} **(B, D)**. **(E)** The inhibitory effects of NaHS on I_{to} channels were not changed by pretreatment with Ver or Tha. **(F)** The inhibitory effects of NaHS on I_{to} channels in cardiomyocytes with or without calcium exhaustion were consistent. NaHS, NaHS 50 μM; Ver, verapamil 20 μM; Ver + Tha, verapamil 20 μM + thapsigargin 2 μM. Values are means ± SEM. $^{**}p < 0.01$ *versus* the vehicle group; $^{\#}p < 0.05$, $^{\#\#}p < 0.01$ *versus* the Ver group; $^{+}p < 0.05$, $^{++}p < 0.01$ *versus* the Ver + Tha group.

peaked in 3 min after injection (Fig. 10D). Myocardial infarction itself caused a decrease in blood pressure (Fig. 10D). Interestingly, both NaHS and Regitine caused an increase in blood pressure in 30 and 60 min in rats with myocardial infarction in contrast to an earlier transient reduction in blood pressure observed in sham-operated rats (Fig. 10D).

The survival rate of the vehicle-treated group was 65.5% in 2 h after myocardial infarction. NaHS treatment significantly improved survival to 91.7% in 2 h after myocardial infarction at dosages of 25 μmol/kg as compared with the vehicle-treated group ($p = 0.024$) (Fig. 10E). The survival in the lidocaine-treated group was also significantly improved as compared with that of the vehicle-treated group ($p = 0.049$) (Fig. 10E). The survival rate of the vehicle-treated group was 37.9% in 24 h after myocardial infarction. NaHS treatment caused a surprising increase in survival to 70.8% and 81.8% at dosages of 25 and 50 μmol/kg as compared with the vehicle-treated group ($p = 0.017$ and 0.013, respectively) (Fig. 10F). Lidocaine (7.5 mg/kg) also caused a significant increase in survival as compared with the vehicle-treated group ($p = 0.019$). In contrast, Regitine did not cause significant improvement in survival (Fig. 10E, F).

Discussion

This study showed that H_2S was a novel inhibitor for the I_{to} potassium current in rat cardiomyocytes. This sheds some light on the understanding of the role of H_2S in electrophysiology of the heart. However, the mechanisms underlying the multifarious biological role of H_2S remain largely unknown. One of the most challenging questions in H_2S biology is identification of H_2S ''receptors'' (15, 39). To date, it remains unknown about how H_2S can regulate an ion channel. Here, we provide the first evidence for a mechanism underlying H_2S-induced regulation in an ion channel. We recorded I_{to} current in HEK293 cells expressing the wild-type pore-forming subunit of the I_{to} potassium channel, Kv4.2, while no background current was recorded in naive HEK293 cells. In such a system, H_2S caused an inhibition in the I_{to}

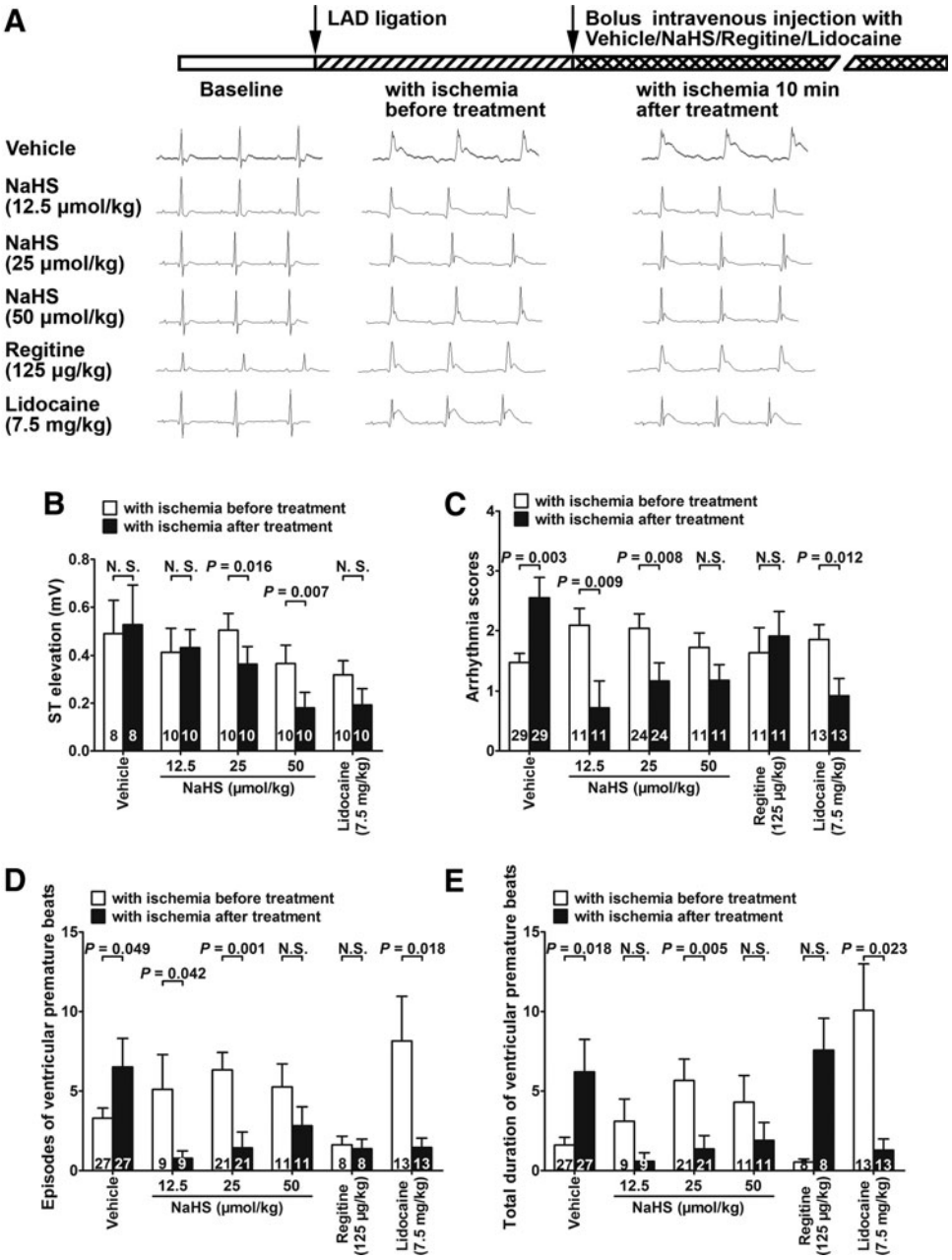

FIG. 9. H_2S is a potent regularizing factor in the rat model of acute myocardial infarction. **(A)** Representative ECG traces of the rats with coronary artery occlusion treated with Vehicle/NaHS/Lidocaine. **(B)** ST segment of ECG in rats with ischemia before and after treatment. **(C)** Arrhythmia scores in rats with ischemia before and after treatment. **(D)** Number of episodes of ventricular premature beats in rats with ischemia before and after treatment. **(E)** Total duration of ventricular premature beats in rats with ischemia before and after treatment. ECG, electrocardiogram.

current. The data indicate that the Kv4.2 subunit serves as a direct target molecule for H_2S regulation.

The next question is how H_2S targets Kv4.2 and regulates its pore-forming function. Some new molecular/atomic mechanisms might be involved in H_2S-induced regulation of I_{to} channels. H_2S interacts with its ''receptor'' with a mechanism beyond the typical ligand-receptor docking (39). We have recently shown that a disulfide bond contained in the intracellular kinase core of the receptor tyrosine kinase serves as a molecular switch for H_2S to regulate the structure and function of VEGFR2 (39). Quantum chemical analysis shows that two H_2S molecules are required to break one disulfide bond molecular switch by nucleophilic attack *via* interaction of the frontier molecular orbitals of the sulfur atom of H_2S and the sulfur atoms of the disulfide bond under attack (39). This previous study led us to search for the potential disulfide bond for H_2S in Kv4.2. Since the crystal structure of Kv4.2 has not yet been determined, it is unknown whether this pore-forming subunit contains some disulfide bond that is labile to H_2S-induced modification. We have to use a fundamental approach to identify the potential target motif for H_2S, that is, creating and expressing a series of recombinant Kv4.2 with all the cysteine residues being mutated one by one. If Kv4.2 contains some disulfide bond for H_2S regulation, certain pairs of cysteine residues would be required for H_2S to exert an inhibitory effect on I_{to} current. In addition, H_2S has been shown to break the disulfide bond and the mutation of either cysteine residues of a disulfide bond also breaks the disulfide bond (39). Interestingly, there was indeed a pair of such cysteine residues in Kv4.2, that is, the Cys320/Cys529 cysteine pair found in this study. We found that the inhibitory effect of H_2S on I_{to} current was blocked by a mutation at

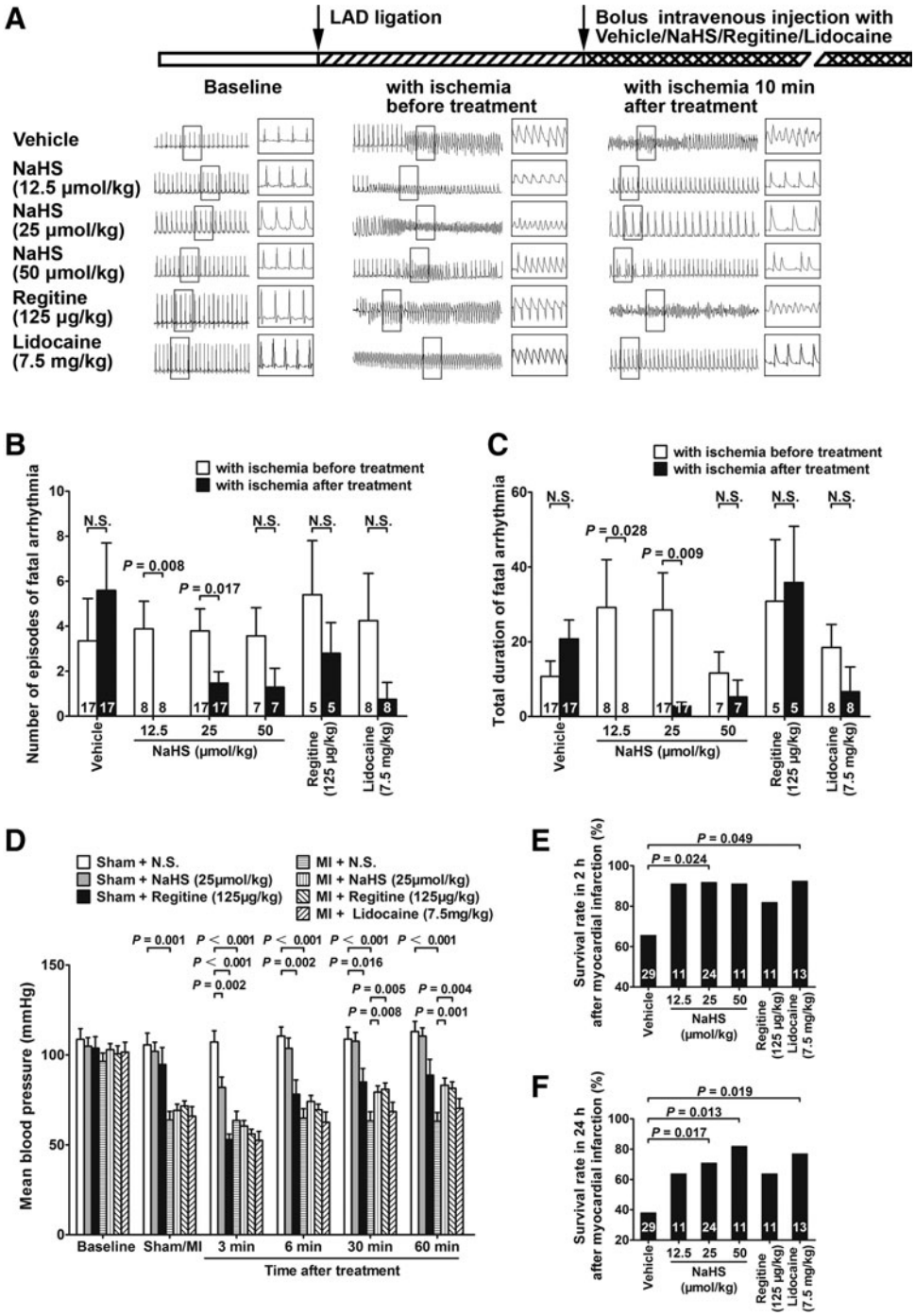

FIG. 10. H_2S treatment provides protection against fatal arrhythmia and improves survival in a rat model of acute myocardial infarction. **(A)** Representative ECG traces of ventricular tachycardia/fibrillation in rats with coronary artery occlusion treated with Vehicle/NaHS/Regitine/Lidocaine. **(B, C)** Number of episodes **(B)** and total time duration **(C)** of ventricular tachycardia/fibrillation in rats with coronary artery occlusion treated with Vehicle/NaHS/Regitine/Lidocaine. **(D)** Blood pressure recorded in rats with sham operation or with coronary artery occlusion treated with Vehicle/NaHS/Regitine/Lidocaine. **(E)** H_2S treatment significantly improves survival rate in 2 h after myocardial infarction. **(F)** H_2S treatment significantly improves survival rate in 24 h after myocardial infarction. Values are mean ± SEM.

either the Cys320 or the Cys529 sites. Double mutation of this cysteine pair resulted in a similar blockade of this H_2S-induced inhibition of the I_{to} current. Our results indicate that the Cys320/Cys529 cysteine pair serves as a specific target motif for H_2S to regulate the channel function of Kv4.2. Using model peptides containing a disulfide bridge linking two peptides (the α and β peptide), each contains a cysteine residue and with a sequence identical to the regions of Cys320 and Cys529 in Kv4.2, H_2S broke this disulfide bond as examined with tandem mass spectrometry. No modification was found in any of the individual amino-acid residues contained in the single peptide α or β. The data support the idea that H_2S targets and cleaves the disulfide bond between a pair of cysteine residues (oxidized form) but does not modify the free $-SH$ groups of a single cysteine residue (reduced form).

Kv4.2 is composed of 630 amino-acid residues, including 16 cysteine residues. What is the function of each of these 16 cysteine residues in regulating the basal conformation and function of Kv4.2? This study showed that an individual mutation of Kv4.2 at Cys390 or Cys484 caused an increase in basal I_{to} current; a mutation of Kv4.2 at Cys132, Cys133, Cys231, Cys236, Cys320, Cys529, or Cys530 caused a decrease in basal I_{to} current; a mutation of Kv4.2 at Cys503,

Cys583, or Cys588 did not change basal I_{to} current; and a mutation of Kv4.2 at Cys111, Cys209, and Cys221 destroyed the channel (without membrane expression and basal I_{to} current). Moreover, H_2S caused different effects on these mutant channels: an unexpected increase in I_{to} current in Kv4.2 units with a mutation at Cys132; a decrease in I_{to} current with a mutation at Cys133, Cys231, Cys236, Cys390, Cys484, Cys503, Cys530, Cys583, or Cys588; and no effect in Kv4.2 with mutations at Cys320 or Cys529. The data demonstrate that 13 out of 16 cysteine residues (except Cys503, Cys583, and Cys588) in Kv4.2 have different roles in regulating the basal channel function of Kv4.2. Future studies are required to further clarify the precise role of each cysteine residues in the conformation and function of Kv4.2.

The linkage between the inhibition on I_{to} potassium channels and the regularizing effect of H_2S remains to be further investigated. The density of I_{to} potassium channels in epicardial myocytes is much higher than that in the endocardial myocytes. This results in a significant difference in the velocity of phase 1 repolarization of action potential in the cardiomyocytes between different layers of myocardium, which is the main mechanism underlying transmural dispersion of repolarization (TDR). In fact, we also observed a significant difference in I_{to} current between epicardial myocytes and endocardial myocytes. Much larger I_{to} in epicardial myocytes causes a much faster phase 1 repolarization and a shorter APD as compared with that of the endocardial myocytes. This difference in repolarization timing of cardiomyocytes from different layers of myocardium is the electrophysiological basis for TDR. It has been shown that ischemia-induced expansion in TDR increases the incidence of arrhythmia (42). In this study, H_2S-induced inhibition in I_{to} was more pronounced in the epicardial myocytes than that in the endocardial myocytes. This reduces the difference in the velocity of phase 1 repolarization of action potential between epicardial myocytes and endocardial myocytes, thereby synchronizing the repolarization process of these two kinds of cardiomyocytes. This might also contribute to a reduction in the incidence of arrhythmia.

The current data suggest a new approach to regulate the electrophysiological property of the cardiomyocytes by regulating the I_{to} channels in cardiac diseases. This idea is supported by a prominent regularizing effect of H_2S treatment against ischemia-induced arrhythmia, including premature beats and ventricular tachycardia and fibrillation in the acute phase of myocardial infarction in a rat model of coronary artery ligation. H_2S treatment also dramatically increased survival in 2 and 24 h after myocardial infarction.

We have previously shown that H_2S does not exert any effect on the K_{ATP} channels in cardiomyocytes at physiologically relevant dosages (37). In this study, H_2S showed no effect on the I_{K1} channels nor on the I_{Na} channels in cardiomyocytes. H_2S specifically inhibited the I_{to} channels. It is well established that the I_{K1} channels regulate the resting potential (17), while the I_{to} channels regulate the velocity of phase 1 repolarization of cardiomyocytes (31, 36). However, I_{Na} channels regulate the velocity and amplitude of depolarization of the action potential (7, 41). This may explain why H_2S decreased the maximal velocity of repolarization and extended the APD but did not affect the resting potential or phase 0 depolarization of the action potential in epicardial myocytes. In fact, H_2S shortened APD_{10} but not $APD_{10–20}$, $APD_{20–50}$, or $APD_{50–90}$. This gives rise to the idea that H_2S-induced extension of the action potential and the refractory period is secondary to an inhibition on I_{to} channels. Here, we provide the first piece of evidence that H_2S can regulate a potassium channel in the cardiomyocytes and this may prompt further research efforts to investigate the role of H_2S in regulation of other potassium channels in the heart.

In contrast to the new role of H_2S in the potassium channels in the cardiomyocytes found in this study, the role of H_2S in the potassium channels in vascular smooth muscle cells has been reported by several independent groups. For example, H_2S treatment has been shown to open the K_{ATP} channels in vascular smooth muscle cells (24). Contradictory evidence is provided by Jackson-Weaver *et al.*, who show that H_2S-induced vasodilatation and hyperpolarization of the vascular smooth muscle cells are not blocked by the K_{ATP} channel inhibitor, glibenclamide (20). Similarly, Streeter *et al.* find that H_2S-induced relaxation of middle cerebral arteries is partly mediated by an inhibition of L-type calcium channels and some unknown potassium channels but not the K_{ATP}, K_{Ca}, K_V, or K_{ir} subtypes (35).

It is obvious that the subtypes of the potassium channels in the cardiomyocytes are distinguished from those in the vascular smooth muscle. The potassium channels in the cardiomyocytes have a unique role in regulating the function of the heart. In particular, the potassium channels are essential in the control of cardiac rhythm and may also serve as drug targets for treating cardiac arrhythmia. We showed here that H_2S treatment is worthy to be further explored as a new potential approach for treating fatal arrhythmia in the critical time window between heart attack and PCI. Indeed, future clinical studies are required to validate the translational value of H_2S treatment in human myocardial infarction. In fact, lidocaine also showed significant regularizing effects in our rat model of myocardial infarction. Lidocaine acts with a different mechanism, that is, an inhibition of the phase 0 depolarization of the action potentials of fast response cells, including cardiomyocytes and neurons. Lidocaine decreases excitability of the cardiomyocytes, thereby inhibiting the generation and transmission of the ectopic pacemakers in myocardial infarction. However, lidocaine also inhibits the generation of action potentials in the neurons in both the central and peripheral nervous system (10, 22). This might cause narcotism, which could become fatal in the acute phase of myocardial infarction. Future clinical studies are required to compare the efficacy and safety of H_2S donor and the current drug lidocaine in treating fatal arrhythmia after acute myocardial infarction. It is worthy of notice that intravenous administration of both NaHS and a known vasodilator, Regitine, caused a transient hypotensive effect in sham-operated rats. In contrast, both NaHS and Regitine caused an increase in blood pressure in rats with myocardial infarction as compared with that treated with vehicle. However, NaHS but not Regitine provided a protection against arrhythmia. These data suggest that H_2S-induced protection against cardiac arrhythmia is not dependent on its potential hypotensive effect and is due to a direct action on the heart.

In addition, ECG showed immediate ST segment elevations in our rat model of myocardial infarction and H_2S treatment immediately decreased ST segment elevations. ST segment elevation has been considered one of the diagnostic criteria for acute myocardial infarction (26). It usually represents the injury current that occurred between injured myocardium and the surrounding noninfarcted myocardium.

H_2S-induced decrease in ST segment elevations may reflect a decrease in injury current.

Indeed, the mechanisms additional to an inhibition of the I_{to} potassium channels may also be involved in H_2S-induced protection against acute myocardial infarction. For example, H_2S improves cardiac function by promoting angiogenesis in mice with transverse aortic constriction (30). In pressure overload-induced heart failure in mice, H_2S provides protection by upregulation of endothelial nitric oxide synthase (23). In addition, we have previously reported that H_2S exerts an inhibition on the L-type calcium channels and the calcium transient, and a negative inotropic effect in the cardiomyocytes (37). These effects are observed within a few minutes after H_2S administration. Both the calcium antagonism and the negative inotropic effects have been shown to provide protection against ischemia-induced arrhythmia (13, 19). In this context, it could not be excluded that H_2S may show some regularizing effects by an inhibition on the L-type calcium channels. H_2S may act through both the calcium channels and the potassium channels to protect the heart against ischemia-induced arrhythmia. Actually, we also examined the role of intracellular calcium in H_2S-induced regulation of I_{to} channels. In the cardiomyocytes with calcium exhaustion, H_2S still showed a significant inhibition on the I_{to} current. The data suggest that H_2S-induced inhibition on I_{to} channels is independent of intracellular calcium.

On the other hand, the I_{K1} channels are essential for regulating the resting membrane potential in cardiomyocytes and have a role in the regulation of myocardium excitability and occurrence of cardiac arrhythmia (5, 18). Therefore, the I_{K1} channels may also serve as a target for potential drugs to treat arrhythmia. However, in this study, H_2S treatment has no effect on the I_{K1} channels. These data do not support the idea that the I_{K1} channels may be involved in the regularizing effects of H_2S in acute myocardial infarction.

Indeed, other H_2S effects such as a protection against cardiomyocytes apoptosis (43) may also contribute to increased survival after myocardial infarction. In addition, H_2S have been found as a proangiogenic factor to stimulate angiogenesis (3), which may also provide protection against chronic myocardial ischemia. However, the very acute protection provided by H_2S in 2 h after myocardial infarction could not be ascribed to the proangiogenic role of H_2S.

Taken together, despite the complexity of the mechanisms underlying the effects of H_2S on ion channels in the heart, our *in vivo* experiments indicate that H_2S is a new efficient regularizing factor to treat fatal ventricular arrhythmia in a rat model of myocardial infarction. The study also uncovers the new inhibitory effect of H_2S on the I_{to} channels. The Kv4.2 unit serves as a direct target molecule for H_2S to regulate the function of the I_{to} channels. The Cys320/Cys529 disulfide bond is an intrinsic requisite motif that is labile to H_2S-induced regulation for the conformation and function of Kv4.2. Future clinical studies are required to examine the translational value of H_2S in treating fatal arrhythmia during the critical time window between a heart attack and PCI.

Materials and Methods

Expression vectors

The pore-forming subunit Kv4.2 (*KCND2, NM-012281.2*) and the auxiliary subunit KChIP2 (*KCNIP2, NM-1731927*) of the human I_{to} potassium channel were purchased from OriGene (Rockville, MD; catalogue No. RG215266/RG219447/RC203823). Kv4.2 is a GFP-tagged ORF clone of potassium voltage-gated channel. KChIP2 is an Myc-DDK-tagged ORF clone of K_v channel interacting protein 2. They are transfection-ready DNAs. We chose pIRES-hrGFP-1a as an expression vector, because this contained an IRES between the multiple cloning site and hrGFP, allowing the expression of our gene of interest, that is, KChIP2 to be monitored at the single-cell level due to expression of hrGFP on the same transcript.

Site-directed mutation of Kv4.2

Site-directed mutation of selected cysteine residues of the wild-type Kv4.2 gene was performed by using the QuikChange Site-Directed Mutagenesis kit (Stratagene, LaJolla, CA) according to the manufacturer's instructions. Briefly, each single-site mutant replaced cysteine residues of the Kv4.2 subunit with an alanine residue. A double-site mutated mutant (*i.e.*, Kv4.2-C320A-C529A) was introduced on the top of the Kv4.2-C320A mutant with the use of the previously mentioned mutagenic primer pair for the Kv4.2-C529A mutagenesis. All constructs were verified by sequencing. All 16 cysteine residues contained in Kv4.2 were individually substituted with an alanine to yield a series of vectors expressing mutant Kv4.2, that is, Kv4.2-C111A, Kv4.2-C132A, Kv4.2-C133A, Kv4.2-C209A, Kv4.2-C221A, Kv4.2-C231A, Kv4.2-C236A, Kv4.2-C320A, Kv4.2-C390A, Kv4.2-C484A, Kv4.2-C503A, Kv4.2-C529A, Kv4.2-C530A, Kv4.2-C563A, Kv4.2-C583A, and Kv4.2-C588A. (Fig. 5, and Supplementary Figs. S2 and S3). In addition, a double mutation was created by replacing both Cys320 and Cys529 with an alanine to a vector expressing Kv4.2-C320A-C529A. All constructs were verified by sequencing.

Cell culture and transfection of the I_{to} channel subunits

HEK293 cells were grown in Dulbecco's modified Eagle's medium (Wako, Tokyo, Japan) supplemented with 10% fetal bovine serum (Gibco, Grand Island, NY), 10% $NaHCO_3$, and 10× L-glumax and maintained at 37°C in a humidified 5% CO_2 incubator. Transient transfection of Kv4.2 or its mutant cDNA with or without KChIP2 in a 1:1 molar ratio into HEK293 cells was performed using FuGENE HD (Roche Molecular Biochemicals, Basel, Switzerland) according to the manufacturer's instructions. KChIP2 is the auxiliary subunit that modifies the function of the pore-forming subunit Kv4.2 (32). Though the KChIP2 subunit alone does not function as a channel, it facilitates the opening of Kv4.2 by modifying the conformation of Kv4.2. Such a modification may change the response of Kv4.2 to some regulating factors such as H_2S. In the cardiomyocytes, Kv4.2 is conjugated with KChIP2 and the potential regulation of H_2S on Kv4.2 actually occurs in such a channel complex, including the pore-forming subunit and the auxiliary subunit. Therefore, we examined the regulation of H_2S on Kv4.2 function in its conjugated form. On the other hand, the H_2S effects were also recorded in the cells transfected with Kv4.2 or its mutant cDNAs alone without KChIP2 to examine whether the H_2S effects are independent of the auxiliary subunit. For electrophysiological recording, the cells were transfected in 35 mm dishes (Corning, Corning, NY) using 4 μl FuGENE HD mixed with 2 μg of total plasmids.

Mass spectrometry

Model chemicals containing a disulfide bond such as Cys–Cys and a synthesized tetradecapeptide that contains an S–S bond between two Cys residues that are located in the central of two heptapeptides synthesized according to the sequence of the residues surround Cys320 and Cys529 of Kv4.2. The tetradecapeptide containing a disulfide bridge linking two peptides (α and β peptide) was synthesized by Glbiochem (Shanghai, China) using trityl (Trt) and methoxybenzyl (Mob) as cysteine-protecting groups to oxidize one of the two cysteine residues in β peptide. Therefore, the disulfide bridge can be formed between two specific cysteine residues in α and β peptide. The model chemicals were individually treated with NaHS (1:5 molar ratio) at room temperature for various time points, and mass spectrometry (MS) analysis of the model chemicals was performed using QSTAR XL mass spectrometer (Applied Biosystem Co., Waltham, MA) in the positive ion mode. Ion spray voltage used for electrospray ionization (ESI) was 2 kV, and high-purity nitrogen gas was used as collision gas for CID in MS analysis on selected MS ions.

Confocal microscopy

The transfected HEK293 cells with GFP fluorescence were seeded in confocal-specific dishes and washed with phosphate-buffered saline. The cells were examined at 488 nm with a confocal laser scanning microscope Zeiss LSM710 (Zeiss, Jena, Germany) that was equipped with an ArKr and an HeNe laser generator.

Isolation of cardiomyocytes

Ventricular myocytes were obtained from hearts of Sprague–Dawley (SD) rats by enzymatic dissociation. All rats were anesthetized with 6% chloral hydrate (0.5 ml/100 g, i.p.). The hearts were rapidly removed and mounted on the Langendorff apparatus for retrograde perfusion. The heart was retroperfused through the aorta with oxygenated Ca^{2+}-free Tyrode's solution at 37°C for 5 min. Then, the heart was perfused with collagenase solution containing 0.5 mg/ml collagenase typeII (Worthington Biochemical Co, Lakewood, NJ), 0.1 mg/ml protease type XIV (Sigma Chemical Co., St Louis, MO), and 1 mg/ml bovine serum albumin (Sigma Chemical Co.) for 15 min. The ventricular myocytes were then dissected as the epicardial and endocardial parts, cut into pieces, and stirred in 37°C Krebs buffer (KB) solution. Then, the isolated cells were washed with 1 m*M* $CaCl_2$ for 10 min, and they were examined with an inverted microscope (Zeiss, Gottingen, Germany). Rod-shaped cells with clear striations without spontaneous contraction were used for further studies. All solutions were gassed with 95% O_2 and 5% CO_2.

Current-clamp recording for action potential

Using an EPC 10 double amplifier (HEKA Elektronic, Lambrecht, Germany), action potential (AP) of epicardial myocytes was recorded in a current-clamp mode with hyperpolarizing current pulses that are two-fold of the threshold stimulation. Isolated myocytes were transferred to a small chamber placed on the stage of an inverted microscope (Zeiss). The chamber was continuously perfused at a constant rate (1.8 ml/min) with Tyrode's solution and maintained at 25°C. Microelectrodes were pulled on a P-97 puller (Sutter Instruments, Novato, CA) and fire polished to 3–5 MΩ resistance. Liquid junction potential was corrected, and a gigaohm seal was formed. Series resistance was compensated by 80%–85%. Data were analyzed using mini-analysis crack and Clampfit version 10.2 software (Axon Instruments, Foster City, CA) and fitted with Origin 8 (OriginLab Corporation, Northampton, MA). The time and maximal velocity of depolarization or repolarization of AP were analyzed with the Clampfit version 10.2 software (Axon Instruments). Then, APD corresponding to APD_{10}, APD_{20}, APD_{50}, and APD_{90} (10%, 20%, 50%, and 90% repolarization), $APD_{10–20}$ (from 10% to 20% repolarization), $APD_{20–50}$ (from 20% to 50%repolarization), and $APD_{20–50}$ (from 50% to 90% repolarization) were measured. To examine the refractory period, the cells were stimulated with a train of eight basal stimulates with an equal interval of 1000 ms followed by one conditional stimulate (premature action potential) with evenly decreasing intervals beginning at 500 ms.

Voltage-clamp recording for I_{to}

Whole-cell patch clamp technique was used to measure I_{to} currents at room temperature (25°C) with the usage of an EPC 10 double amplifier (HEKA Elektronic, Lambrecht, Germany). Isolated myocytes or cultured HEK293 cells transfected with wild-type Kv4.2 or mutant Kv4.2 with or without KChIP2 were transferred to a small chamber placed on the stage of an inverted microscope (Zeiss). The chamber was continuously perfused at a constant rate (1.8 ml/min) with the extracellular solution for I_{to} recording and maintained at 35°C. Microelectrodes were pulled on a P-97 puller (Sutter Instruments) and fire polished to 3–5 MΩ resistance. Liquid junction potential was corrected, and a gigaohm seal was formed. Series resistance was compensated by 80%–85%. Currents were filtered at 5 kHz and digitized at 10 kHz. Data were analyzed using mini-analysis crack and Clampfit version 10.2 software (Axon Instruments) and fitted with Origin 8 (OriginLab Corporation). I_{to} was elicited by depolarizing voltage steps (500 ms) from −30 to +60 mV (0.1 Hz) with a holding potential of −80 mV, and a 20 ms prepulse was applied to −40 mV to inactivate the fast Na^+ current. *I–V* relationship of I_{to} was obtained by plotting the peak current amplitude *versus* the potential. As the peak current was composed of two major currents, including I_{to} and I_{ss} in rat ventricular myocytes, I_{to} was defined as: $I_{to} = I_{peak} - I_{ss}$. Data were normalized as current densities by dividing current amplitude by whole-cell capacitance (pA/pF). NaHS (50 μM) was added to obtain *I–V* relationship curves of I_{to}/I_{ss} in both epicardial and endocardial myocytes. In addition, NaHS 25, 50, 100, and 200 μM was acquired to acquire time- and dose-dependent curves of I_{to}.

To acquire the steady-state active curves, I_{to} was induced with 500 ms depolarizing pulses between −100 and +60 mV from a holding potential of −80 mV. The steady-state inactivation of I_{to} was examined using a two-pulse protocol containing a 1000 ms prepulse between −100 and +60 mV and a subsequent 500 ms test pulse to +60 mV from a holding potential of −80 mV with an interval of 10 ms. To examine the recovery curves of I_{to}, cardiomyocytes were stimulated with a double pulse protocol that contains a 500 ms

conditioning pulse to 0 mV followed by a 200 ms test pulse to 0 mV from a holding potential of −80 mV with increasing intervals between 10 and 200 ms (29). All the experiments mentioned earlier were performed in the presence or absence of NaHS (50 μM).

Voltage-clamp recording for I_{K1}

With a holding potential of −80 mV, I_{K1} was elicited by depolarizing voltage steps (500 ms) from −120 to 0 mV (0.1 Hz) in the presence or absence of NaHS (100 μM). The control group was treated with vehicle (Supplementary Fig. S4A).

Voltage-clamp recording for I_{Na}

I_{Na} was induced with 30 ms depolarizing pulses between −100 and +40 mV from a holding potential of −100 mV. Both *I–V* relationship and time-dependent curves of I_{Na} were examined in the presence or absence of NaHS (100 and 200 μM). The control group was treated with vehicle (Supplementary Fig. S4B and C).

Effect of $[Ca^{2+}]_i$ on H_2S-induced inhibition on I_{to} in the cardiomyocytes

After incubation with the L-type calcium channel blocker, verapamil (20 μM), and/or the SEARCA blocker, thapsigargin (2 μM) (8), *I-V* relationship, and time-dependent curves of I_{to} in myocytes were examined in the absence or presence of NaHS at 50 μM.

Solutions

The Tyrode's solution (m*M*): 137 NaCl, 5.0 KCl, 1.2 $MgSO_4$, 1.8 $CaCl_2$, 0.5 NaH_2PO_4, 10 glucose, and 10 HEPES; pH was adjusted to 7.4 with NaOH. Ca^{2+}-free solution was deprived of $CaCl_2$. The KB solution (m*M*): 70 KOH, 40 KCl, 20 KH_2PO_4, 50 glutamic acid, 3 $MgCl_2$, 20 taurine, 0.5 EGTA, 10 HEPES, and 10 glucose; pH was adjusted to 7.4 with KOH. The pipette solution (m*M*) for action potential recording: 135 KCl, 3 $MgCl_2$, 10 EGTA, and 10 HEPES; pH was adjusted to 7.4 with KOH. The extracellular solution (m*M*) for I_{to} recording: 140 NaCl, 4 KCl, 1.5 $CaCl_2$, 1 $MgCl_2$, 0.5 $CdCl_2$, 5 HEPES, and 10 glucose; pH was adjusted to 7.4 with NaOH. The pipette solution (m*M*) for I_{to} recording: 140 KCl, 1 $MgCl_2$, 5 K_2ATP, 5 EGTA, and 10 HEPES; pH was adjusted to 7.4 with KOH. The extracellular solution (m*M*) for I_{K1} recording: 145 Choline Cl, 5 KCl, 1 $MgCl_2$, 5 EGTA, 10 HEPES, and 10 glucose; pH was adjusted to 7.4 with KOH. The pipette solution (m*M*) for I_{K1} recording: 140 KCl, 1 $CaCl_2$, 5 K_2ATP, 10 EGTA, and 10 HEPES; pH was adjusted to 7.4 with KOH. The extracellular solution (m*M*) for I_{Na} recording: 120 Choline Cl, 25 NaCl, 4 CsCl, 1.8 $CaCl_2$, 1 $MgCl_2$, 2 $CoCl_2$, 5 HEPES, and 10 glucose; pH was adjusted to 7.4 with CsOH. The pipette solution (m*M*) for I_{Na} recording: 140 CsCl, 10 NaCl, 5 Na_2ATP, 5 EGTA, and 5 HEPES; pH was adjusted to 7.4 with CsOH.

Animals

Male SD rats (200–250 g) were obtained from the Department of Experimental Animals, Chinese Academy of Sciences. All animal procedures conformed to the *Guide for the Care and Use of Laboratory Animals* published by the National Institutes of Health in the United States and was approved by the Ethics Committee of Experimental Research, Fudan University Shanghai Medical College.

Ventricular arrhythmia induced by acute myocardial infarction

Animals were anesthetized by 6% chloral hydrate by an intraperitoneal injection (0.5 ml/kg). Acute myocardial infarction models were made by occluding the LAD artery at 2 mm inferior to the left auricle using a 6-0 silk suture. Male SD rats were randomly divided into five groups: the vehicle-treated group; the NaHS-treated groups at dosages of 12.5, 25, and 50 μmol/kg group, respectively; and the lidocaine-treated group at a dosage of 7.5 mg/kg ($n = 10$–17). At 10 min after acute myocardial infarction, NaHS, lidocaine, or vehicle was administered with a bolus injection *via* the femoral vein. ECG was recorded with standard limb lead II for 5 min at baseline, for 10 min after myocardial infarction, and for 2 h after treatment. Severity of ventricular arrhythmias was assessed according to a scoring system designed by Curtis and Walker (11): 0 = no ventricular premature beats, ventricular tachycardia, or ventricular fibrillation; 1 = ventricular premature beats; 2 = 1–4 episodes of ventricular tachycardia; 3 = ≥5 episodes of ventricular tachycardia or 1 episode of ventricular fibrillation or both; 4 = 2–4 episodes of ventricular fibrillation; and 5 = ≥5 episodes of ventricular fibrillation or death.

Statistical analysis

All data are expressed as means ± SEM. Determination of statistical significance between two groups was accomplished using Student's *t*-test. One-way analysis of variance (ANOVA) was used for multiple-group comparison, followed by *post hoc* Tukey's test. In addition, arrhythmia scores were analyzed with ANOVA for repeated measurement design data and survival rates were tested by chi-square test. The significance level was set at $p < 0.05$.

Acknowledgments

This work was supported by grants from the National Natural Science Foundation of China (81230003, 31471088), the Ministry of Science and Technology (2012ZX09501001-001-002) of China, the Science and Technology Commission of Shanghai Municipality (12JC1400700), and a key laboratory program of the Education Commission of Shanghai Municipality (ZDSYS14005).

Author Disclosure Statement

No competing financial interests exist.

References

1. Angelini P. Sudden cardiac death: do we know what we are talking about? *Circulation* 105: E182–E182, 2002.
2. Bazzani C, Mioni C, Ferrazza G, Cainazzo MM, Bertolini A, and Guarini S. Involvement of the central nervous system in the protective effect of melanocortins in myocardial ischemia/reperfusion injury. *Resuscitation* 52: 109–115, 2002.
3. Cai WJ, Wang MJ, Moore PK, Jin HM, Yao T, and Zhu YC. The novel proangiogenic effect of hydrogen sulfide is dependent on Akt phosphorylation. *Cardiovasc Res* 76: 29–40, 2007.
4. Cannon CP, Gibson CM, Lambrew CT, Shoultz DA, Levy D, French WJ, Gore JM, Weaver WD, Rogers WJ, and

Tiefenbrunn AJ. Relationship of symptom-onset-to-balloon time and door-to-balloon time with mortality in patients undergoing angioplasty for acute myocardial infarction. *JAMA* 283: 2941–2947, 2000.
5. Carmeliet E. Function and pharmacology of the potassium channels in the heart and vessels. *Arch Mal Coeur Vaiss* 85: 465–471, 1992.
6. Carmeliet E. K^+ channels and control of ventricular repolarization in the heart. *Fundam Clin Pharmacol* 7: 19–28, 1993.
7. Catterall W. Voltage-dependent gating of sodium channels: correlating structure and function. *Trends Neurosci* 9: 7–10, 1986.
8. Chen L, Xu Y, Li W, Wu H, Luo Z, Li X, Huang F, Young C, Liu Z, and Zhou S. The novel compound liguzinediol exerts positive inotropic effects in isolated rat heart via sarcoplasmic reticulum Ca^{2+} ATPase-dependent mechanism. *Life Sci* 91: 402–408, 2012.
9. Cheng JH and Kodama I. Two components of delayed rectifier K^+ current in heart: molecular basis, functional diversity, and contribution to repolarization. *Acta Pharmacol Sin* 25: 137–145, 2004.
10. Chikharev VN, Mal'tsev VA, and Rozenshtraukh LV. Lidocaine action on the ion currents of normal and depolarized myocardial fibers in membrane potential fixation. *Biull Vsesoiuznogo Kardiol Nauchn Tsentra AMN SSSR* 4: 58–66, 1981.
11. Curtis MJ and Walker MJ. Quantification of arrhythmias using scoring systems: an examination of seven scores in an in vivo model of regional myocardial ischemia. *Cardiovasc Res* 22: 656–665, 1988.
12. Dhamoon AS and Jalife J. The inward rectifier current (I_{k1}) controls cardiac excitability and is involved in arrhythmogenesis. *Heart Rhythm* 2: 316–324, 2005.
13. Gelpi RJ, Mosca SM, Rinaldi GJ, Kosoglov A, and Cingolani HE. Effect of calcium antagonism on contractile behavior of canine hearts. *Am J Physiol* 244: H378–H386, 1983.
14. Giudicessi JR and Ackerman MJ. Potassium-channel mutations and cardiac arrhythmias-diagnosis and therapy. *Nat Rev Cardiol* 9: 319–332, 2012.
15. Hoefer IE. Something is rotten in the state of angiogenesis–H_2S as gaseous stimulator of angiogenesis. *Cardiovasc Res* 76: 1–2, 2007.
16. Hondeghem LM and Katzung BG. Unifying molecular model for interaction of antiarrhythmic drugs with cardiac sodium channels: application to quinidine and lidocaine. *Pro West Pharmacol Soc* 20: 253–256, 1977.
17. Hutter OF and Noble D. Rectifying properties of heart muscle. *Nature* 188: 495, 1960.
18. Ion channels in the cardiovascular system. *Science* 257: 271–273, 1992.
19. Ishii K, Taira N, and Yanagisawa T. Differential antagonism by Bay k 8644, a dihydropyridine calcium agonist, of the negative inotropic effects of nifedipine, verapamil, diltiazem and manganese ions in canine ventricular muscle. *Br J Pharmacol* 84: 577–584, 1985.
20. Jackson-Weaver O, Paredes DA, Gonzalez Bosc LV, Walker BR, and Kanagy NL. Intermittent hypoxia in rats increases myogenic tone through loss of hydrogen sulfide activation of large-conductance Ca^{2+}-activated potassium channels. *Circ Res* 108: 1439–1447, 2011.
21. Johnson CC and Miner PF. The occurrence of arrhythmias in acute myocardial infarctions. *Dis Chest* 33: 414–422, 1958.
22. Khodorova A, Meissner K, Leeson S, and Strichartz GR. Lidocaine selectively blocks abnormal impulses arising from noninactivating Na^+ channels. *Muscle Nerve* 24: 634–647, 2001.
23. Kondo K, Bhushan S, King AL, Prabhu SD, Hamid T, Koenig S, Murohara T, Predmore BL, Gojon G, Sr., Gojon G, Jr., Wang R, Karusula N, Nicholson CK, Calvert JW, and Lefer DJ. H_2S protects against pressure overload-induced heart failure via upregulation of endothelial nitric oxide synthase. *Circulation* 127: 1116–1127, 2013.
24. Li L, Rose P, Moore PK, and Cho A. Hydrogen sulfide and cell signaling. *Annu Rev Pharmacol and Toxicol* 51: 169–187, 2011.
25. Mustafa AK, Sikka G, Gazi SK, Steppan J, Jung SM, Bhunia AK, Barodka VM, Gazi FK, Barrow RK, Wang R, Amzel LM, Berkowitz DE, and Snyder SH. Hydrogen sulfide as endothelium-derived hyperpolarizing factor sulfhydrates potassium channels. *Circ Res* 109: 1259–1268, 2011.
26. Nielsen BL. ST-segment elevation in acute myocardial infarction. Prognostic importance. *Circulation* 48: 338–345, 1973.
27. Noma A. ATP-regulated K^+ channels in cardiac muscle. *Nature* 305: 147–148, 1983.
28. Odoherty M, Tayler DI, Quinn E, Vincent R, and Chamberlain DA. 500 patients with myocardial-infarction monitored within one hour of symptoms. *Br Med J* 286: 1405–1408, 1983.
29. Okubo K, Takahashi T, Sekiguchi F, Kanaoka D, Matsunami M, Ohkubo T, Yamazaki J, Fukushima N, Yoshida S, and Kawabata A. Inhibition of T-type calcium channels and hydrogen sulfide-forming enzyme reverses paclitaxel-evoked neuropathic hyperalgesia in rats. *Neuroscience* 188: 148–156, 2011.
30. Polhemus DJ, Kondo K, Bhushan S, Bir SC, Kevil CG, Murohara T, Lefer DJ, and Calvert JW. Hydrogen sulfide attenuates cardiac dysfunction after heart failure via induction of angiogenesis. *Circ Heart Fail* 6: 1077–1086, 2013.
31. Priebe L and Beuckelmann DJ. Simulation study of cellular electric properties in heart failure. *Circ Res* 82: 1206–1223, 1998.
32. Radicke S, Vaquero M, Caballero R, Gomez R, Nunez L, Tamargo J, Ravens U, Wettwer E, and Delpon E. Effects of MiRP1 and DPP6 beta-subunits on the blockade induced by flecainide of Kv4.3/KChIP2 channels. *Br J Pharmacol* 154: 774–786, 2008.
33. Rosequist CC. Current standards and guidelines for cardiopulmonary-resuscitation and emergency cardiac care. *Heart Lung* 16: 408–418, 1987.
34. Shih HT. Anatomy of the action-potential in the heart. *Tex Heart Inst J* 21: 30–41, 1994.
35. Streeter E, Hart J, and Badoer E. An investigation of the mechanisms of hydrogen sulfide-induced vasorelaxation in rat middle cerebral arteries. *Naunyn Schmiedebergs Arch Pharmacol* 385: 991–1002, 2012.
36. Sun X and Wang HS. Role of the transient outward current (I_{to}) in shaping canine ventricular action potential—a dynamic clamp study. *J Physiol* 564: 411–419, 2005.
37. Sun YG, Cao YX, Wang WW, Ma SF, Yao T, and Zhu YC. Hydrogen sulphide is an inhibitor of L-type calcium channels and mechanical contraction in rat cardiomyocytes. *Cardiovasc Res* 79: 632–641, 2008.

38. Tamargo J, Caballero R, Gomez R, Valenzuela C, and Delpon E. Pharmacology of cardiac potassium channels. *Cardiovasc Res* 62: 9–33, 2004.
39. Tao BB, Liu SY, Zhang CC, Fu W, Cai WJ, Wang Y, Shen Q, Wang MJ, Chen Y, Zhang LJ, Zhu YZ, and Zhu YC. VEGFR2 functions as an H_2S-targeting receptor protein kinase with its novel cys1045-cys1024 disulfide bond serving as a specific molecular switch for hydrogen sulfide actions in vascular endothelial cells. *Antioxid Redox Signal* 19: 448–464, 2013.
40. Tian XY, Wong WT, Sayed N, Luo J, Tsang SY, Bian ZX, Lu Y, Cheang WS, Yao X, Chen ZY, and Huang Y. NaHS relaxes rat cerebral artery in vitro via inhibition of L-type voltage-sensitive Ca^{2+} channel. *Pharmacol Res* 65: 239–246, 2012.
41. Weidmann S. The effect of the cardiac membrane potential on the rapid availability of the sodium-carrying system. *J Physiol* 127: 213–224, 1955.
42. Yan GX, Joshi A, Guo D, Hlaing T, Martin J, Xu X, and Kowey PR. Phase 2 reentry as a trigger to initiate ventricular fibrillation during early acute myocardial ischemia. *Circulation* 110: 1036–1041, 2004.
43. Yao LL, Huang XW, Wang YG, Cao YX, Zhang CC, and Zhu YC. Hydrogen sulfide protects cardiomyocytes from hypoxia/reoxygenation-induced apoptosis by preventing GSK-3 beta-dependent opening of mPTP. *Am J Physiol Heart Circ Physiol* 298: H1310–H1319, 2010.
44. Zhao W, Zhang J, Lu Y, and Wang R. The vasorelaxant effect of H_2S as a novel endogenous gaseous K_{ATP} channel opener. *EMBO J* 20: 6008–6016, 2001.
45. Zheng ZJ, Croft JB, Giles WH, and Mensah GA. Sudden cardiac death in the United States, 1989 to 1998. *Circulation* 104: 2158–2163, 2001.

Address correspondence to:
Prof. Yi-Chun Zhu
Department of Physiology and Pathophysiology
Fudan University Shanghai Medical College
138 Yi Xue Yuan Road
Shanghai 200032
China

E-mail: yczhu@shmu.edu.cn

Date of first submission to ARS Central, August 18, 2014; date of final revised submission, January 30, 2015; date of acceptance, February 24, 2015.

Abbreviations Used

ANOVA = analysis of variance
APD = action potential durations
cAMP = 3′,5′-cyclic adenosine monophosphate
cGMP = 3′,5′-cyclic guanosine monophosphate
CID = collision-induced dissociation
$+dV/dt_{max}$ = maximal velocity of phrase 0 depolarization
$-dV/dt_{max}$ = maximal velocity of repolarization
ECG = electrocardiogram
EGTA = ethylene glycol-bis-(2-aminoethylether)-*N*,*N*,*N*′,*N*′-tetraacetic acid
ESI = electrospray ionization
GFP = green fluorescent protein
H_2S = hydrogen sulfide
HEPES = 4-(2-hydroxyethyl)piperazine-1-ethanesulfonic acid
I_K = delayed rectifier K^+ channel
I_{K1} = inward rectifier K^+ channel
I_{Na} = sodium channel
IRES = internal ribosome entry sites
I_{ss} = steady-state outward current
I_{to} = transient outward K^+ channels
K_{ATP} channel = ATP-sensitive K^+ channel
KB = Krebs buffer
K_{Ca} = Ca^{2+} activated K^+ channel
KChIP2 = K_v channel interacting protein 2
LAD = left anterior descending
MS = mass spectrometry
NaHS = sodium hydrosulfide
ORF = open reading frame
PCI = percutaneous coronary intervention
SD = Sprague-Dawley
SEM = standard error of the mean
TDR = transmural dispersion of repolarization
VEGFR2 = vascular endothelial growth factor type 2 receptor